Three distinct Holocene intervals of stalagmite deposition and non-deposition revealed in NW Madagascar, and their paleoclimate inferences

Voarintsoa, Ny Riavo G.[1*], L. Bruce Railsback[1], George A. Brook[2], Lixin Wang[2], Gayatri Kathayat[3], Hai Cheng[3,4], Xianglei Li[3], R. Lawrence Edwards[4], Rakotondrazafy Amos Fety Michel[5], Madison Razanatseheno Marie Olga[5]

[1] Department of Geology, University of Georgia, Athens, GA 30602-2501 U.S.A.
[2] Department of Geography, University of Georgia, Athens, Georgia, 30602-2502 U.S.A.
[3] Institute of Global Environmental Change, Xi'an Jiaotong University, Xi'an, Shaanxi 710049, P.R. China
[4] Department of Earth Sciences, University of Minnesota, Minneapolis, Minnesota 55455, U.S.A.
[5] Department of Geology, University of Antananarivo, Madagascar

*Correspondence to: Ny Riavo Voarintsoa (nv1@uga.edu or nyriavony@gmail.com)

ABSTRACT

Petrographic features, mineralogy, and stable isotopes from two stalagmites collected from Anjohibe and Anjokipoty caves allow distinction of three intervals of the Holocene in NW Madagascar. The Malagasy early Holocene (between c. 9.8 and 7.8 ka) and late Holocene (after c. 1.6 ka) intervals (MEHI and MLHI, respectively) record evidence of stalagmite deposition. The Malagasy middle Holocene interval (MMHI, between c. 7.8 ka and 1.6 ka), however, is marked by a depositional hiatus lasting for c. 6500 years.

Deposition of Stalagmites ANJB-2 and MAJ-5 from Anjohibe and Anjokipoty caves, respectively, during the MEHI and the MLHI suggests that these caves were sufficiently supplied with water to allow stalagmite formation. These MEHI and MLHI intervals may have been comparatively wet. In contrast, the long-term depositional hiatus likely suggests that the MMHI was relatively drier than the MEHI and the MLHI. This dry condition could have influenced the amount of water supplied to the cave, and thus prevented formation of the stalagmites.

The alternating “wet/dry/wet” during each of these Holocene intervals could be generally linked to the long-term migration of the Inter-Tropical Convergence Zone (ITCZ). When the ITCZ’s mean position is farther south, NW Madagascar experiences wetter conditions, such as during the MEHI and MLHI, and when it moves north, NW Madagascar climate becomes drier, such as

during the MMHI. A similar wet/dry/wet succession during the Holocene has been reported in neighboring locations, such as southeastern Africa.

Stable isotope records also suggest that although the MEHI and MLHI were wetter, the stronger correlation between $\delta^{18}O$ and $\delta^{13}C$ suggest that the early Holocene vegetation closely responded to changes in climate. In contrast, the weaker correlation between $\delta^{18}O$ and $\delta^{13}C$ and the positive shift in $\delta^{13}C$ suggest that the late Holocene vegetation was controlled by something other than climate, and the plausible explanation for such changes is the practice of swidden agriculture, as reported in previous literature.

Beyond these three subdivisions, the evidence of the 8.2 ka event in the stalagmite records also suggests that climate in Madagascar was sensitive to abrupt climate changes, such as the abrupt influx of the Laurentide Ice Sheet meltwater to the North Atlantic. The freshwater influx into the N. Atlantic, known to have weakened the Atlantic Meridional Overturning Circulation (AMOC), also led to an enhanced temperature gradient between the two hemispheres, i.e. cold NH and warm SH, shifting the mean position of the ITCZ further south. This brought wet conditions in the SH monsoon regions, such as NW Madagascar, and dry conditions in the NH monsoon regions, including the Asian Monsoon and the East Asian Summer Monsoon.

1. Introduction

Although much is known about Holocene climate change worldwide (Mayewski et al., 2004; Wanner and Ritz, 2011; Wanner et al., 2011; 2015), high-resolution climate data for the Holocene period is still regionally limited in the Southern Hemisphere (SH) (e.g., Wanner et al., 2008; Marcott et al., 2013; Wanner et al., 2015). This uneven distribution of data hinders our understanding of the spatio-temporal characteristics of Holocene climate change, and the forcings involved. For example, some of these forcings would have an influence on Inter-Tropical Convergence Zone (ITCZ) behavior and monsoonal response in low- to mid-latitude regions (e.g., Wanner et al., 2015; Talento and Barreiro, 2016). The island of Madagascar, in the southwest Indian Ocean (Fig. 1a), is seasonally visited by the ITCZ with a karst region crossing latitudinal belts (Fig. 1c). Thus, it is a natural laboratory to study changes in the ITCZ over time. New records from Madagascar could fill gaps in paleoclimate reconstruction in the SH that might help refine paleoclimate simulations, which in turn could provide better understanding of the global circulation and the land–atmosphere–ocean interaction during the Holocene.

In this paper, we present multiproxy records (stable isotopes, petrography, mineralogy, variability of layer-specific width, or LSW) from stalagmites from Anjohibe and Anjokipoty caves. Stalagmites are used because of their potential to store significant climatic information (e.g., Fairchild and Baker, 2012, p. 9–10), and in Anjohibe Cave, recent studies have shown the replicability of paleoclimate records from stalagmites (e.g., Burns et al., 2016).

Two stalagmites were investigated, and these allowed us to characterize Holocene climate change in NW Madagascar. First, we developed a record of climate change from the multiproxy data. With a better understanding of Madagascar's paleoclimate, we then investigated possible climate drivers of tropical climate change to draw a more comprehensive conclusion on the major factors controlling the hydrological cycle in NW Madagascar and surrounding regions during the Holocene.

2. Setting

2.1. Stalagmites and their setting

Stalagmites are secondary cave deposits that are $CaCO_3$ precipitates from cave dripwater. Calcium carbonate precipitation occurs mainly by CO_2 degassing, which increases the pH of the dripwater and thus increases the concentration of CO_3^{2-}. In some cases, evaporation may also contribute to increased Ca^{2+} and/or CO_3^{2-} concentration in dripwater. CO_2 degassing occurs when high-PCO_2 water from the epikarst encounters low-PCO_2 cave air. Evaporation occurs when humidity inside the cave is relatively low. The fundamental equation for stalagmite deposition is shown in Eq. 1.

$$Ca^{2+}_{(aq)} + 2HCO^{-}_{3\,(aq)} \rightleftharpoons CaCO_{3\,(s)} + CO_{2\,(g)} + H_2O_{(l)} \text{ (Eq. 1)}$$

Growth and non-growth of stalagmites depends on conditions that affect the reaction of Eq. 1 above. An increase in Ca^{2+} drives the equation to the right (towards precipitation) and an increase in CO_2 of the cave air and/or H_2O drives it to the left (towards dissolution). All components of the equation are influenced by the supply of water to the cave, which is generally climate-dependent. More water enters the cave during warm/rainy seasons than during cold/dry seasons. Stalagmites will form when cave dripwater is saturated with respect to calcite and/or aragonite. If the water passes through the bedrock too quickly to dissolve significant carbonate rock, and/or enters the cave and reaches the stalagmite too quickly to degas significant CO_2, it will not be saturated with respect to $CaCO_3$, inhibiting stalagmite formation. Stalagmite growth will slow as dripwater declines and will stop entirely if flow ceases. Vegetation provides CO_2 to the soil via root respiration so the vegetation cover above the cave and the type of vegetation can promote or limit stalagmite growth. Overall, the karst hydrological system plays a crucial role in the deposition and non-deposition of stalagmites, and this is closely linked to changes in local and regional environment and climate.

2.2. Regional environmental setting

Stalagmites ANJB-2 and MAJ-5 were collected from Anjohibe and Anjokipoty caves, respectively, in the Majunga region of NW Madagascar (Fig. 1). Sediments and fossils from these caves have already provided many insights about the paleoenvironmental and archaeological history of NW Madagascar (e.g., Burney et al., 1997, 2004; Brook et al., 1999; Gommery et al., 2011; Jungers et al., 2008; Vasey et al., 2013; Burns et al., 2016; Voarintsoa et al., 2017b).

Anjohibe (S15° 32' 33.3"; E046° 53' 07.4") and Anjokipoty (S15° 34' 42.2"; E046° 44' 03.7") are about 16.5 km apart (Fig. 1c). Their location in the zone visited by the ITCZ (e.g., Nassor and Jury, 1998) makes them ideal sites to test the hypothesis that latitudinal migration of the ITCZ influenced the Holocene climate of NW Madagascar (e.g., Chiang and Bitz, 2005; Broccoli et al., 2006; Chiang and Friedman, 2012; Schneider et al., 2014). The ITCZ brings north or northwesterly monsoon winds to Madagascar during austral summers, in a pattern that the Service Météorologique of Madagascar calls the “Malagasy monsoon”. Majunga has a tropical savanna climate (Aw) according to the Köppen-Geiger climate classification, with a distinct wet summer (from October to April) and dry winter (May-September). The mean annual rainfall is around 1160 mm. The mean maximum temperature in November, the hottest month in the summer, is about 32°C. The mean minimum temperature in July, the coldest month of the dry winter, is about 18°C (Fig. 1b).

*2.3.*Climate of Madagascar

The climate of Madagascar is unique because of its varied topography and its position in the Indian Ocean. Some scientists refer Madagascar as a "laboratory" for paleoecological study (e.g., Burney, 1997) because it is not only susceptible to several climatic forcing mechanisms but also an island with recent anthropogenic interaction, living imprints in the geological records (e.g., Burney et al., 2003, 2004; Matsumoto and Burney, 1994; Crowley and Samonds, 2013; Burns et al., 2016; Voarintsoa et al., 2017b). Its climate has been reviewed in several recent works (e.g., Jury, 2003; DGM, 2008, Douglas and Zinke, 2015, p. 281-299; Voarintsoa et al., 2017b, p.138-139; Scroxton et al., 2017). Regionally distinct rainfall gradients from east to west and from north to south are evident across the country (Jury, 2003; Dewar and Richard, 2007), and these are linked to easterly trade-winds in winter (May-October) and northwesterly tropical storms in summer, respectively. The Malagasy monsoon is modulated by the seasonal north-south migration of the ITCZ, which is the main driver of austral summer rainfall in Madagascar. The ITCZ's mean position has shifted northward or southward depending on the global climate conditions, but most generally it migrates towards the Earth's warmer hemisphere (Frierson and Hwang, 2012; Kang et al., 2008; McGee et al., 2014; Sachs et al., 2009). A relationship between this long-term migration of the ITCZ and climate in Madagascar was reported in NW Madagascar between c. 370 CE and 800 CE (see Fig, 8 of Voarintsoa et al., 2017b).

Beyond ITCZ, climate of Madagascar is also influenced by changes in Indian Ocean sea surface temperatures (SST) (Zinke et al., 2004; see also Kunhert et al., 2014) and changes in SST of the adjacent current off southwestern Madagascar, the Aghulas Current (Lutjeharms, 2006; Beal et al., 2011; Zinke et al., 2014). The most immediate signal is the Indian Ocean Dipole (IOD), or Indian Ocean Zonal Mode (Li et al., 2003). IOD-like patterns have been proposed as possible contributors to Holocene climate variability in tropical Indian Ocean (Abram et al., 2009; Tierney et al., 2013). IOD is as a coupled atmosphere-ocean mode in the tropical Indian Ocean (e.g., Saji et al., 1999; Webster et al., 1999; Brown et al., 2009; Yagamata et al., 2004; Behera et al., 2013). It is characterized by a reversal of the climatological SST gradient and winds across the Indian Ocean basin (Saji et al., 1999; Webster et al., 1999; Abram et al., 2007; Brown et al., 2009). A positive IOD event starts with anomalous SST cooling along the Sumatra-Java coast in the eastern

Indian Ocean (Abram et al., 2007, 2008), along with positive SST anomaly in the western part of the basin (e.g., Saji et al., 1999; Abram et al., 2007). Such positive IOD events are observed to result in increased precipitation, sometimes causing devastating floods, over East Africa (Black et al., 2003; Saji et al., 1999; Webster et al., 1999; Saji and Yagamata, 2003; Weller and Cai, 2014). Such events have also enhanced precipitation over the northern part of India, the Bay of Bengal, Indochina, and southern part of China in 1994 (e.g., Behera et al., 1999; Guan and Yamagata, 2003; Saji and Yagamata, 2003). In the eastern Indian Ocean, a positive IOD is found to intensify El-Niño related drought, often as severe droughts, over Indonesia (Webster et al., 1999; Weller and Cai, 2014). It is however, important to note that the relationship between IOD and El-Nino Southern Oscillation (ENSO) is still debated. While some researchers found no relationships (e.g., Saji et al., 1999; Li et al., 2003; Lee et al., 2008), others found some relationships (e.g., Brown et al., 2009; Schott et al., 2009; Shinoda et al., 2004; Venzke et al., 2000; Abram et al., 2008; Saji and Yagamata, 2003; Meyers et al., 2007).

Apart from the coral study of Zinke et al. (2004) and the stalagmite study of Scroxton et al. (2017), very little is known about the effect of the IOD on Madagascar. One objective of this stalagmite study is to better understand how such mechanisms influenced climate in Madagascar during the Holocene.

2.4. The Holocene in NW Madagascar

Little is hitherto known about Holocene climate change in NW Madagascar nor about the major drivers of long-term climatic changes there. Most paleoclimate information from this region covers the last two millennia with more focus on the anthropogenic effects on the Malagasy ecosystems (e.g., Crowley and Samonds, 2013; Burns et al., 2016; Voarintsoa et al., 2017b). This is because several studies show that megafaunal extinctions in Madagascar coincide with the arrival of humans around 2-3 ka BP (e.g., see Table 1 of Virah-Sawmy et al., 2010; MacPhee and Burney, 1991; Burney et al., 1997; Crowley, 2010). There are even fewer long-term paleoclimate records for the NW region, with only sediments from Lake Mitsinjo (3,500 yr. BP; Matsumoto and Burney, 1994) and stalagmites from Anjohibe Cave (40,000 yr. BP; Burney et al. 1997) providing records of more than 3 kyr. Even though these records provided useful information about the paleoenvironmental changes in NW Madagascar, their linkages to global climatic change, such as the linkages to the ITCZ, are not yet fully understood.

3. Methods

3.1. Radiometric dating

A total of 22 samples were drilled from Stalagmite ANJB-2 and 9 samples for Stalagmite MAJ-5 for U-series dating (Table S1 and S2). Each sample is a long (~5 to 20 mm), narrow (~1-2mm), and shallow (~1 mm) trench, allowing us to extract 50–250 mg of $CaCO_3$ powder. We followed the chemical procedures described in Edwards et al. (1987) and Shen et al. (2002) when separating uranium and thorium. U/Th measurements were performed on the multi-collector ICP-MS of the University of Minnesota, USA and on a similar instrument in the Stable Isotopes Laboratory of Xi'an, in Jiaotong, China. Instrument details are provided in Cheng et al. (2013). Corrected ^{230}Th ages assume an initial $^{230}Th/^{232}Th$ atomic ratio of $4.4 \pm 2.2 \times 10^{-6}$. This is the ratio for "bulk earth" or crustal material at secular equilibrium with a $^{232}Th/^{238}U$ value of 3.8. The uncertainty in the "bulk earth" value is assumed to be ±50% (see footnotes to Table S1 and S2). The error in the final "corrected age" incorporates this uncertainty. The radiometric data are reported as year BP, where BP is Before Present, and "Present" is A.D. 1950. Stalagmite chronologies were constructed using the StalAge1.0 algorithm of Scholz and Hoffman (2011) and Scholz et al. (2012), an algorithm using a Monte-Carlo simulation designed to construct speleothem age models. The algorithm can identify major and minor outliers and age inversions. The StalAge scripts were run on the statistics program R version 3.2.2 (2015-08-14). The age models were adjusted considering hiatal surfaces identified in the samples, using the approach of Railsback et al. (2013; see their Fig. 9).

3.2. Petrography and mineralogy

Petrography and mineralogy of the two stalagmites were investigated 1) by examining both the polished surfaces and the scanned images of the sectioned stalagmites, and by identifying any diagenetic fabrics (e.g., Zhang et al., 2014) that could potentially affect stable isotope values, 2) by observing eleven oversized thin sections (3x2 in) under the Leitz Laborlux 12 Pol microscope and the Leica DMLP equipped with QCapture in the Sedimentary

Geochemistry Lab at the University of Georgia, 3) by using scanning electron microscopy (SEM) to better understand the mineralogical fabrics at locations of interest (Fig. S13), and 4) by analyzing about 30–100 mg of powdered spelean layers (n=15) on a Bruker D8 X-ray Diffractometer in the Department of Geology, University of Georgia. For calcite and aragonite identification, we used CoKα radiation at a 2θ angle between 20° and 60°.

Layer-specific width (LSW) of clearly-defined layers was measured at selected locations on the stalagmite polished surfaces (Fig. S4; Sletten et al., 2013; Railsback et al., 2014; Voarintsoa et al., 2017b). LSW is the horizontal distance between two points on the flanks of the stalagmite where convexity is greatest. It is the width near the top of the stalagmite when the layer being examined was deposited. LSW is measured at right angles to the growth axis of the stalagmite; it is the horizontal distance between points on the layer growth surface becomes tangent to a line inclined at 35° to the growth axis (Fig. S4). LSW may vary along the length of the stalagmite, with smaller values suggesting drier conditions and larger values wetter conditions.

3.3. Stable isotopes

Stable isotope samples of 50–100 μg were manually drilled along the stalagmite's growth layers at the crest. The trench size is very small (1.5 x 0.5 x 0.5 mm). Since a small mixture of calcite and aragonite could potentially change the $\delta^{18}O$ and $\delta^{13}C$ of the measured spelean layers (see for example Frisia et al., 2002), drilling and sample extraction was carefully done on individually discrete layers using the smallest drill-bit head (SSW-HP-1/4) to avoid potential mixing between calcite and aragonite. The polished surface of the two stalagmites were examined to see if features of diagenetic alteration are present (see for example fig. 2 of Zhang et al., 2014), but none was found. During sampling, the mineralogy at the crest, where stable isotope samples were extracted, was recorded for future mineralogical correction.

Aragonite oxygen and carbon isotopic corrections were performed to compensate for aragonite's inherent fractionation of heavier isotopes (e.g., Romanek et al., 1992; Kim et al., 2007; McMillan et al., 2005) and to remove the mineralogical bias in isotopic interpretation between calcite and aragonite. The correction consists of subtracting 0.8‰ for $\delta^{18}O$ (Kim and O'Neil, 1997; Tarutani et al., 1969; Kim et al., 2007; Zhang et al., 2014) and 1.7 ‰ for $\delta^{13}C$

(Rubinson and Clayton, 1969; Romanek et al., 1992) for the aragonite as has been done previously (e.g., Holmgren et al., 2003; Sletten et al., 2013; Liang et al., 2015; Railsback et al., 2016; Voarintsoa et al., 2017a) as shown in equations 2 and 3 below (where $R_{A/C}$ is the aragonite percentage if not 100%).

$$\delta^{18}O_{corr.} \text{ (‰, VPDB)} = \delta^{18}O_{uncorr.} \text{ (‰, VPDB)} – [R_{A/C} \times 0.8 \text{ (‰, VPDB)}] \text{ (Eq. 2)}$$

$$\delta^{13}C_{corr.} \text{ (‰, VPDB)} = \delta^{13}C_{uncorr.} \text{ (‰, VPDB)} – [R_{A/C} \times 1.7 \text{ (‰, VPDB)}] \text{ (Eq. 3)}$$

Supplementary Figures S6–S8 show both the corrected and uncorrected isotopic records.

For the analytical methods, oxygen and carbon isotope ratios were measured using the Finnigan MAT-253 mass spectrometer fitted with the Kiel IV Carbonate Device of the Xi'an Stable Isotope Laboratory in China (ANJB-2; n=654) and using the Delta V Plus at 50°C fitted with the GasBench-IRMS machine of the Alabama Stable Isotope Laboratory in USA (MAJ-5; n=286). Analytical procedures using the MAT 253 are identical to those described in Dykoski et al. (2005), with isotopic measurement errors of less than 0.1 ‰ for both $\delta^{13}C$ and $\delta^{18}O$. Analytical methods and procedures using the GasBench-IRMS machine are identical to those described in Skrzypek and Paul (2006), Paul and Skrzypek (2007), and Lambert and Aharon (2011), with ±0.1 ‰ errors for both $\delta^{13}C$ and $\delta^{18}O$. In both techniques, the results are reported relative to Vienna PeeDee Belemnite (VPDB) and with standardization relative to NBS19. An inter-lab comparison of the isotopic results was conducted, and it involved replicating every tenth sample of Stalagmite MAJ-5 at both labs. This exercise showed a strong correlation between the lab results (Fig. S5).

4. Results

4.1. Radiometric data

Results from radiometric analyses of the two stalagmites are presented in Tables S1 and S2. Corrected ^{230}Th ages suggest that Stalagmite ANJB-2 was deposited between c. 8977±50 and c. 161±64 yr. BP, and Stalagmite MAJ-5 was deposited between c. 9796±64 and c. 150±24 yr. BP. These ages collectively indicate stalagmite deposition at the beginning (between 9.8 and 7.8 ka BP) and at the end of the Holocene (after c. 1.6 ka BP). In both stalagmites, the older ages have small 2σ errors and they generally fall in correct stratigraphic order, except sample ANJB-2-120 and its replicate ANJB-2-120R, which were not used because of the sample's high porosity and high detritals content. In contrast, many of the younger ages have larger uncertainties. This is mainly because many of the younger samples have very low uranium concentration and the detrital thorium concentration is also high, similar to what Dorale et al. (2004) reported. We also understand that the value for initial ^{230}Th correction, i.e. the initial ^{230}Th/^{232}Th atomic ratio of 4.4 ± 2.2 × 10^{-6} for a bulk earth with a ^{232}Th/^{238}U value of 3.8, in these samples could have slightly altered the ^{230}Th age of these younger samples, leading to larger uncertainties (such as discussed in Lachniet et al., 2012). We encountered similar problems while working on other younger samples from the same cave, but we compared the stable isotope profile with other published records using isochron corrections, and results did not differ significantly (see Fig. 9 of Voarintsoa et al., 2017b). Since this work does not focus on decadal or centennial interpretation of the Late Holocene stable isotope data, additional chronology adjustment has not been made, and we used the chronology from StalAge to construct the time series. However, in Figures 5 and 6, age uncertainties are given below the stable isotope profiles so that comparisons with other records can accommodate these uncertainties.

The key finding from our age and petrographic data for the two stalagmites is that they suggest that there were three distinct intervals of growth and non-growth during the Holocene (Figs. 2–4, 7). The information suggesting this includes: (1) $CaCO_3$ deposition between c. 9.8 and 7.8 ka B.P., (2) a long depositional hiatus between c. 7.8 and 1.6 ka B.P., and (3) resumption of $CaCO_3$ deposition after c. 1.6 ka B.P. In the rest of the paper, we will refer to these intervals as the Malagasy Early Holocene Interval (MEHI), Malagasy Mid-Holocene Interval (MMHI), and Malagasy Late Holocene Interval (MLHI), respectively.

*4.2.*Stable isotopes

Raw values of δ^{18}O and δ^{13}C for Stalagmite ANJB-2 range from –8.9 to –2.3‰ (mean = –5.0‰), and from –11.0 to +5.2‰ (mean = –4.2‰), respectively, relative to VPDB. Raw values of δ^{18}O and δ^{13}C for Stalagmite MAJ-5 range from –8.8 to –0.9‰ (mean = –4.9‰), and from –9.4 to +2.6‰ (mean = –4.4‰), respectively, relative to VPDB. Mean δ^{18}O and δ^{13}C values are distinguishable between the MEHI and the MLHI. In both stalagmites, the amplitude of δ^{18}O fluctuations was fairly constant throughout the Holocene; whereas the $\delta^{13}C$ profile shows a dramatic shift toward higher values (i.e. from -10.9‰ to +3.8‰, VPDB) at c. 1.5 ka BP.

The MEHI and MLHI are isotopically distinct (Fig. 4). The MEHI is characterized by statistically correlated $\delta^{18}O$ and $\delta^{13}C$ (r^2=0.65 and 0.53), and much depleted $\delta^{13}C$ values (c –11.0 to –4.0 ‰). The 8.2 ka event, a widespread cold event in the NH (e.g., Alley et al., 1997), is also apparent in the stalagmite records. Stalagmite $\delta^{18}O$ and $\delta^{13}C$ ratios reach their lowest values of –6.8 and –10.9‰, respectively during that interval (Figs. 5, 12). In contrast to the MEHI, the values of $\delta^{18}O$ and $\delta^{13}C$ during the MLHI are poorly correlated (r^2=0.25 and 0.17), and $\delta^{13}C$ values are more enriched (Figs. 4, 6).

Since Stalagmites ANJB-2 and MAJ-5 were collected from two different caves 16 km apart, discrepancies between the stable isotopes at the same age are expected, suggesting that local conditions could be one of the discrepancy factors. Another potential source for the discrepancy is the larger uncertainty of the younger ages due to low uranium and high detrital concentrations. This U-Th aspect has been a challenge for several young stalagmites (e.g., Dorale et al., 2004; Lachniet et al., 2012) including samples from NW Madagascar (this study). While the utility of speleothems as a climate proxy largely depends on replication of stable isotope values, it is important to note that perfect stable isotope replication can only occur between stalagmites collected from the same cave chamber (e.g., Dong et al., 2010; Burns et al., 2016).

4.3. Mineralogy, petrography, and layer-specific width

In both stalagmites, the hiatus of deposition is characterized by a well-developed Type L surface (Figs. 2, 3, S15). Petrography and mineralogy are distinct before and after this hiatus (Fig. 3). Below the hiatus, laminations are well preserved in both stalagmites. Above the hiatus, laminations are not well-preserved, although noted in some intervals.

In Stalagmite ANJB-2, the layer-specific width varies from 37 to 26.5 mm with a mean of 30 mm. It decreases to 28 mm at the hiatus (Fig. 3). Below the hiatus, mineralogy is dominated by aragonite, although a few thick layers of calcite are also identified. A thin (~2-3 mm) but remarkable layer of white, very soft, and porous aragonite is identified just below the hiatus (Fig. S15). This layer is covered by a very thin layer of dirty carbonate. Above the hiatus, mineralogy is also composed of calcite and aragonite, with calcite dominant, and the calcite layers contain macro-cavities that are mostly off-axis macroholes (Shtober-Zisu et al., 2012).

In Stalagmite MAJ-5, LSW varies from 50 to 22 mm with a mean of 35.5 mm. It decreases to 22 mm at the hiatus (Fig. 3). Below the hiatus, mineralogy is a mixture of calcite and aragonite. Above the hiatus, mineralogy is mainly calcite and macro-cavities are also present throughout that upper part of the stalagmite.

4.4. Summary of results

The various records from Stalagmites ANJB-2 and MAJ-5 suggest three distinct climate/hydrological intervals of the Holocene. The MEHI (c. 9.8 to 7.8 ka BP), with evidence of stalagmite deposition, is characterized by statistically correlated $\delta^{18}O$ and $\delta^{13}C$ (r^2=0.65 and 0.53) and more negative $\delta^{13}C$ values (c. –11.0 to –4.0 ‰). The MMHI (c. 7.8 to 1.6 ka BP) is marked by a long-term hiatus in deposition, which is preceded by a well developed Type L surface in both Stalagmite ANJB-2 and MAJ-5 (Figs. 3, S15). The Type L surface is observed as an upward narrowing of the stalagmite's width and layer thickness. It is particularly well developed in Stalagmite MAJ-5 (Fig. S15). In Stalagmite ANJB-2, the hiatus at the Type L surface is preceded by a c. 3 mm thick layer of highly porous, very soft, and fibrous white crystals of aragonite (the only aragonite with such properties). This aragonite is topped by a thin and well-defined layer of detrital materials (Fig. S15), further supporting the presence of a hiatus. Finally, the MLHI (after c. 1.6 ka BP) is characterized by poorly correlated $\delta^{18}O$ and $\delta^{13}C$ (r^2=0.25–0.17). This interval is additionally marked by a shift in $\delta^{13}C$ toward higher values (Figs. 4, 6).

5. Discussion

5.1. Paleoclimate significance of stalagmite growth and non-growth: implications for paleohydrology

Growth and non-growth of stalagmites depends on several factors linked to water availability, which is largely determined by climate (more water during warm/rainy seasons and less water during cold/dry seasons). Water is the main dissolution and transporting agent for most chemicals in speleothems. Cave hydrology varies significantly over time in response to climate, and this variability influences the formation or dissolution of $CaCO_3$. In this regard, calcium carbonate does not form if there is little or no water entering the cave, or if there is too much (see Sect. 2.1). Absence of groundwater recharge most typically occurs during extremely dry conditions, whereas excessive water input to the cave occurs during extremely wet conditions. In the latter scenario, water is undersaturated and flow rates are too fast to allow degassing. Often, water availability is reflected in the extent of vegetation above and around the cave, as plants require soil moisture or shallow groundwater to survive and propagate, and this contributes to the stalagmites' processes of formation. The linkage of stalagmites' growth and non-growth to cave dripwater and soil CO_2 is broadly influenced by changes in climate.

Major hiatuses in stalagmite deposition could be marked by a variety of features, including the presence of erosional surfaces, chalkification, dirt bands/detrital layers, offsetting of the growth axis, and/or sometimes by color changes (e.g., Holmgren et al., 1995; Dutton et al., 2009; Railsback et al., 2013; Railsback et al., 2015; Voarintsoa et al., 2017a). Railsback et al. (2013) were specifically able to identify significant features in stalagmites that allow distinction between non-deposition during extremely wet (Type E surfaces) and non-deposition during extremely dry conditions (Type L surfaces; Fig. 3). Physical properties of stalagmites that are evidence of extreme dry and wet events are summarized in Table 1 of Railsback et al. (2013) and the mechanism is explained in their Figure 5.

Type E surfaces are layer-bounding surfaces between two spelean layers when the underlying layers show evidence of truncation. The truncation results from dissolution or erosion (thus the name "E") of previously-formed layers of stalagmites by abundant undersaturated water. Type E surfaces are commonly capped with a layer of calcite (Railsback et al., 2013). This mineralogical trend is not surprising as calcite commonly forms under wetter conditions (e.g., Murray, 1954; Pobeguin, 1965; Siegel, 1965; Thrailkill, 1971; Cabrol and Coudray, 1982; Railsback et al. 1994; Frisia et al., 2002). Additionally, non-carbonate detrital materials are commonly abundant with varying grain size (i.e., from silt- to sand-size; Railsback et al., 2013).

Type L surfaces, on the other hand, are layer-bounding surfaces where the layers became narrower upward and thinner towards the flanks of the stalagmite. Decreases in layer thickness and stalagmites width of the stalagmites upward are indications of lessening deposition (thus the name “L”; Railsback et al., 2013). Aragonite is a very common mineralogy below a Type L surface, especially in warmer settings. Layers of aragonite commonly form under drier conditions (Murray, 1954; Pobeguin, 1965; Siegel, 1965; Thrailkill, 1971; Cabrol and Coudray, 1982; Railsback et al., 1994; Frisia et al., 2002). Non-carbonate detrital materials are scarce, and if present, they tend to form a very thin horizon of very fine dust material (Railsback et al., 2013). Identification of Type L surfaces is aided by measuring the LSW (e.g., Sletten et al., 2013; Railsback et al., 2014), an approach that is also performed in this study (Fig. S4).

5.2. Holocene climate in NW Madagascar

Although the specific boundaries between the Early, Mid, and Late Holocene have been proposed for global application (Walker et al., 2012; Head and Gibbard, 2015), their use is still spatially limited (e.g., Wanner et al., 2015). The age models and petrographic features of Stalagmites ANJB-2 and MAJ-5 suggest three distinct but different Holocene climate intervals (MEHI, MMHI, and MLHI; see Sect. 4.1) in NW Madagascar. These intervals are illustrated in the sketches of Figure 4. In this paper, these Malagasy intervals are intended not to argue against the previously proposed intervals of the Holocene (Walker et al., 2012; Head and Gibbard, 2015). Instead, they are presented to aid discussion of the available records. For comparison, the intervals are shown in Fig. 7d.

5.2.1. Malagasy early Holocene interval (c. 9.8 –7.8 ka BP)

Stalagmite deposition during the early Holocene suggests that the chambers, where stalagmites ANJB-2 and MAJ-5 were collected, were sufficiently supplied with water to allow $CaCO_3$ precipitation, in accord with Eq.1. This in turn implies relatively wet conditions that could indicate longer summer rainy seasons relative to modern climate, or wet years in NW Madagascar (see Supplementary Text 4 and Fig. 8). The correlative $\delta^{13}C$ and $\delta^{18}O$ values further suggest that vegetation consistently responded to changes in moisture availability, which in turn was dependent on climate.

One striking aspect of the Stalagmite ANJB-2 $\delta^{18}O$ and $\delta^{13}C$ records is that they parallel the $\delta^{18}O$ of the Greenland ice core records at c 8.2 ka BP (Figs. 5 and 12). An X-ray diffraction spectrum for this period, at 195–202 mm from the top of the stalagmite, suggests that the mineralogy at 8.2 ka BP is 100% calcite (Figs. S14, S16–S17). This calcite is not a diagenetic product of aragonite for three reasons. First, the laminations in the thick layer of calcite were not altered (Figs. S16–S17). Second, the polished surface of the stalagmite shows no evidence of fiber relicts and textural ghosts such as observed in Juxtlahuaca Cave in southwestern Mexico (Lachniet et al., 2012) and in Shennong Cave in southeastern China (Zhang et al., 2014). Third, petrographic comparison with known examples of primary and secondary calcite observation under microscope (e.g., Railsback, 2000; Perrin et al., 2014) suggests that there is no strong evidence of aragonite–to–calcite transformation. The decrease in $\delta^{18}O$ and $\delta^{13}C$ values and the presence of calcite mineralogy at the same interval combine to suggest a wet 8.2 ka BP event in NW Madagascar. The 8.2 ka BP event is a prominent cold event in the North Atlantic records and many NH terrestrial records. It may have been triggered by a release of freshwater from the melting Laurentide Ice Sheet into the North Atlantic basin (e.g., Alley et al., 1997; Barber et al., 1999). Freshwater influx to the Atlantic could have altered the Atlantic Meridional Overturning Circulation (AMOC, e.g., Clark et al., 2001), and could eventually have influenced the climate of Madagascar (Sect. 5.5). Our records reveal a strong link between paleoenvironmental changes in Madagascar and abrupt climatic events in the NH records, suggesting causal relationships.

The MEHI terminated when conditions became much drier, as suggested by increasing $\delta^{18}O$ and $\delta^{13}C$ values in Stalagmite ANJB-2, by decreasing LSW of both stalagmites, and by major Type L surfaces in both stalagmites. The thin (c. 3 mm), porous, and white aragonite layer in Stalagmite ANJB-2, a very similar deposit to that described in Niggemann et al. (2003), suggests that the terminal drought was at times severe. Aragonite is a $CaCO_3$ polymorph that forms preferentially under drier conditions (Murray, 1954; Pobeguin, 1965; Siegel, 1965; Thrailkill, 1971; Cabrol and Coudray, 1982; Railsback et al. 1994; Frisia et al., 2002). The porous aragonite layer in Stalagmite ANJB-2 is capped by a very thin layer of non-carbonate, brown detritus, which may have been transported to the stalagmite as an aerosol and accumulated on the dry stalagmite surface over time. Accumulation of the detritus must take place in the absence of dripwater (e.g., Railsback et al., 2013). A shift to drier conditions is also supported by isotopic data from Stalagmite ANJ94-5 from Anjohibe Cave (Wang and Brook, 2013; Wang, 2016) in which relatively low $\delta^{13}C$ and $\delta^{18}O$ values prior to 7600 BP give way to episodically greater values thereafter.

5.2.2. Malagasy mid-Holocene interval (c. 7.8–1.6 ka BP)

The only data we have for the MMHI is the long term (~6.5 ka) depositional hiatus in both stalagmites (Figs. 2–3), that potentially indicate dry conditions. The question is why did neither stalagmite grow during the MMHI? Here, we try to explain the factors and the climatic conditions that may have been responsible for it.

The documented severe dry conditions at the end of the MEHI (see Sect. 5.2.1) could have had a significant influence (1) on the cave hydrological system (e.g., Fig. 5 of Asrat et al., 2007; Bosak, 2010), such as the water conduits (primary or secondary porosity) to the chambers, and (2) on the vegetation cover above the caves, particularly above the chambers where Stalagmites ANJB-2 and MAJ-5 were collected. On one hand, it is possible that the dry conditions late in the MEHI could not only bring lesser water recharge to the cave, but also lowered the hydraulic head, and increased the rate of evapo-transpiration in the vadose zone. This condition possibly allowed more air to penetrate the aquifer, perhaps enhancing prior carbonate precipitation (PCP) in pores and conduits above the caves (e.g., Fairchild and McMillan, 2007; Fairchild et al., 2000; Johnson et al., 2006; Karmann et al., 2007; McDonald et al., 2007). This process must have blocked water moving towards Stalagmites ANJB-2 and MAJ-5. On the other hand, the late MEHI drying trend (Sect. 5.2.1) could have challenged vegetation to grow, and we assume that some areas above Anjohibe and Anjokipoty caves must have been devoid of vegetation. Consequently, biomass activities could have been reduced. Because vegetation contributes CO_2 to the carbonic acid dissolving $CaCO_3$, its absence in certain areas above the cave could decrease the pH of the percolating water, and perhaps dissolution did not occur. Under these conditions, even if water reached the stalagmites, it may not have precipitated carbonate.

Whatever factors were responsible for the long term-depositional hiatus in Stalagmite ANJB-2 and MAJ-5, we believe that the hiatus was caused by disturbances to water catchments that feed the chambers at Anjohibe and Anjokipoty caves. The disturbances could be inherited from the very dry conditions at the end of the MEHI, and/or due to the lack of water supply, perhaps associated with an increase in epikarst ventilation, and/or by the absence of vegetation. Water and vegetation are two components of the karst system that play an important role in $CaCO_3$ dissolution and precipitation (see Eq. 1). Their disturbance may have limited limestone dissolution in the epikarst and then carbonate precipitation in the cave zone.

Other evidence supports the idea of at least episodic dryness during the MMHI. A work on a 2-meter long stalagmite (ANJ94-5) from Anjohibe Cave suggests episodic dryness during the MMHI and a depositional hiatus around the time when Stalagmites ANJB-2 and MAJ-5 stopped growing (Wang and Brook, 2013; Wang, 2016). For regional comparison, dry spells were also felt in Central and Southeastern Madagascar (e.g., Gasse and Van Campo, 1998; Virah-Sawmy et al., 2009).

In summary, several lines of evidence suggest relatively drier climate in NW Madagascar during the MMHI compared to the MEHI. Drier intervals generally imply drier summer seasons with less rainfall (Fig. 8), perhaps reflecting shorter visits by the ITCZ. In this regard, even though the region received rainfall, the necessary conditions could not have been attained to activate the growth of Stalagmites ANJB-2 and MAJ-5, thus the hiatuses.

5.2.3. Malagasy Late Holocene Interval (c. 1.6 ka–present)

Resumption of stalagmite deposition after c. 1.6 ka BP suggests a wetter climate in NW Madagascar with reactivation of the previous epikarst hydrologic system. Conditions must have been similar to those of the early Holocene. Wet conditions between c. 850 and 1100 AD in Stalagmite ANJB-2 and Stalagmite MAJ-5, specifically coincide with glacial advances at northern high latitudes (Holzhauser et al., 2005) and a cooler interval of the Medieval Climate Anomaly, as suggested by a negative temperature Anomaly in the NH (e.g., Büntgen et al., 2011; Mann et al., 1998; Mann and Bradley, 1999, see also Fig. S18). The sudden beginning of stalagmite growth during the MLHI and the large $\delta^{13}C$ shift from depleted to enriched values at c. 1.5 ka BP (Fig. 6), after such long hiatuses may have been associated with changes in vegetation cover above the cave linked to recent human activities (e.g., Burns et al., 2016; Crowley and Samonds, 2013; Crowther et al., 2016; Voarintsoa et al., 2017b). Lower $\delta^{13}C$ values in Stalagmite MAJ-5 after 0.8

ka BP (Fig. 3), compared to higher values in Stalagmite ANJB-2, suggests different conditions in or above the two caves. More human disturbance at one site could account for the different trends, or alternatively changes in cave micro-climate, or in the hydrologic catchments of the two stalagmites.

Although the stalagmite data indicate overall wetter conditions during the last c. 1.6 kyr, there were occasional dry periods, as suggested by several positive peaks in the stalagmite $\delta^{18}O$ records. Drier intervals during the Late Holocene are observed in the Anjohibe data between c. AD 755 and 795 (i.e., 1195–1155 yr. BP; Voarintsoa et al., 2017b). Similar conditions have been recorded in other paleoenvironmental studies, in which a peak drought c. 1300–950 cal BP was reported (Burney, 1987a, b; Burney, 1993; Matsumoto and Burney, 1994; Virah-Sawmy et al., 2009).

5.3. Holocene climate in NW Madagascar: implications for ITCZ dynamics

Figures 7 and 8 depict possible conditions in NW Madagascar during the MEHI, the MMHI, and the MLHI. Figure 9 summarizes the possible forcings mechanisms linked to the latitudinal migration of the ITCZ.

In NW Madagascar, stalagmite deposition during the MEHI and the MLHI could suggest there was sufficient dripwater for stalagmite growth and therefore wetter conditions. This could have been linked to a more southerly mean position of the ITCZ. Factors that could influence the mean position of the ITCZ include changes in insolation (e.g., Haug et al., 2001; Wang et al., 2005; Cruz et al., 2005; Fleitmann et al., 2003, 2007; Schefuß et al., 2005; Suziki, 2011; Kutzbach and Liu, 1997; Partridge et al., 1997; Verschuren et al., 2009; Voarintsoa et al., 2017a) and difference in temperature between the two hemispheres (e.g., Chiang and Bitz, 2005; Broccoli et al., 2006; Chiang and Friedman, 2012; Kang et al., 2008; McGee et al., 2014; Talento and Barreiro, 2016).

In contrast, the depositional hiatuses during the MMHI could suggest drier conditions, and thus a northward migration of the mean ITCZ. It seems to agree with the paleoclimate simulation of Braconnot et al. (2007) of the 6 ka event, suggesting that the NH insolation increased (Braconnot et al., 2000; see also Chiang, 2009). This northward shift in the mean position of the ITCZ is consistent with drier conditions, i.e. weaker South American Summer Monsoon (e.g., Cruz et al., 2005; Seltzer et al., 2000; Wang et al., 2007; but see also Fig. 9 of Zhang et al., 2013) but wetter conditions in the northern tropics (e.g., Dykoski et al., 2005; Fleitmann et al., 2007; Gasse, 2000; Haug et al., 2001; Weldeab et al., 2007; Zhang et al., 2013).

5.4. Regional comparisons

Despite differences in Holocene paleoclimate reconstructions for southern Africa, comparison of the NW Madagascar records with records from neighboring locations (Figs. 10–11; Table S3) shows that the Holocene wet/dry/wet succession reported in this study has also been identified at other locations. For example, hydrogen isotope compositions of the n-C31 alkane in GeoB9307-3 from a 6.51 m long marine sediment core retrieved about 100 km off the Zambezi delta suggest a similar wet/dry/wet climate during Early, Middle, and Late Holocene respectively (Schefuß et al., 2011). Those changes correspond to changes in temperature from ~26.5° to 27.25° to 27°C, respectively, in the Mozambique Channel, as suggested by alkenone SST records from sediment cores MD79257 (Bard et al., 1997; Sonzogni et al., 1998). The Zambezi catchment is specifically relevant here because it is located at the southern boundary of the modern ITCZ, and so has similar climatic setting as NW Madagascar, and its sensitivity to the latitudinal migration of the ITCZ could parallel that of Madagascar. Likewise, temperature reconstruction from the Mozambique Channel could be used to link regional changes in paleorainfall with regional changes in temperature. A general overview of the Holocene climate in the African neighboring locations to Madagascar suggests a roughly consistent wetter and drier climate during the early and middle Holocene, respectively (Fig. 11, Table S3, also see Gasse, 2000; Singarayer and Burrough, 2015). However, Late Holocene paleoclimate reconstructions vary. A single answer to this variability is unlikely, but several overlapping factors, including the latitudinal migration of the ITCZ, changes in ocean oscillations and sea surface temperatures, volcanic aerosols, and anthropogenic influences could have played a major role in such variability (e.g., Nicholson, 1996; Gasse, 2000; Tierney et al., 2008; Truc et al., 2013). Assessing these factors is beyond the scope of this study.

5.5. The 8.2 ka event in Madagascar: linkage to ITCZ and AMOC

The 8.2 ka event was a significant short-lived cooling of the N Atlantic and NH during the Early Holocene (Alley et al., 1997). It is apparent in the ANJB-2 and MAJ-5 stalagmite records as a wet interval (Sect. 5.2.1; Figs. 5, 12). The 8.2 ka event is a known interval of abrupt freshwater influx from the melting Laurentide Ice Sheet into the North Atlantic (Alley et al., 1997; Barber et al., 1999; Kleiven et al., 2008; Carlson et al., 2008; Renssen et al, 2010; Wiersma et al., 2011; Wanner et al., 2015). It is equivalent to the sharp peak of Bond cycle number 5 (Bond et al. 1997, 2001). This influx of meltwater altered the density and salinity of the NADW. Thornalley et al. (2009) report that there was a decrease in NADW salinity to approximately 34 p.s.u. during the Early Holocene.

Understanding the AMOC's influence on Madagascar's hydroclimate could help us better understand global atmospheric and oceanic circulation, particularly in the SH. An increase in the flow of freshwater to the North Atlantic decreases the formation of North Atlantic Deep Water, reducing the meridional heat transport (Barber et al., 1999; Clark et al., 2001; Daley et al., 2011; Vellinga and Wood 2002; Dong and Sutton 2002, 2007; Dahl et al. 2005; Zhang and Delworth 2005; Daley et al., 2011; Renssen et al., 2001). Weakening of the AMOC would ultimately cause a widespread cooling in the NH regions (e.g., Clark et al., 2001; Thomas et al., 2007) but warming in the SH regions (Wiersma et al., 2011; Wiersma and Renssen, 2006). This "cold NH–warm SH" climate response is similar to the "bipolar seesaw" effect, well-known during the last glacial (e.g., Crowley, 1992; Broecker, 1998). The interhemispheric temperature difference between the NH and SH from such effect could be the driver of the southward displacement of the mean position of the ITCZ during the 8.2 ka abrupt cooling event. This in turn could have led to an intensified Malagasy monsoon in NW Madagascar during austral summers, a phenomenon identical to the South American Summer Monsoon identified in Brazil (e.g., Cheng et al., 2009). In contrast, regions in the NH monsoon regions became dry at 8.2 ka BP as the Asian Monsoon and the East Asian Monsoon became weaker (e.g., Wang et al., 2005; Dykoski et al., 2005; Cheng et al., 2009; Liu et al., 2013).

5.6. Beyond the ITCZ: IOD and ENSO influence on Madagascar's climate

Although the ITCZ is the main driver of rainfall availability in Madagascar, recent studies have also suggested the importance of SST changes in the surrounding ocean and teleconnection with other climatic phenomena. Scroxton et al. (2017) linked rainfall changes in eastern Indian Ocean with expansion and contraction of the ITCZ along with positive IOD. Zinke et al. (2004) revealed strong Indian Ocean subtropical dipole events that were in phase with ENSO indices between AD 1880 and 1920, and between 1930 and 1940, and after 1970 in austral summers. Brook et al. (1999, p. 700) suggested linkages between rainfall and ENSO in NW Madagascar since AD 1550, a relationship that is less clear and complicated. This complication could be associated with an unclear or yet a limited understanding of the relationship between IOD and ENSO, which is not yet fully understood (e.g., Saji et al., 1999; Li et al., 2003; Lee et al., 2008 versus Brown et al., 2009; Schott et al., 2009; Shinoda et al., 2004; Venzke et al., 2000; Abram et al., 2008; Saji and Yagamata, 2003; Meyers et al., 2007).

Our understanding of the oceanic and atmospheric circulation is challenged because IOD and ENSO share similar features in the associated SST and precipitation anomalies (e.g., Saji et al., 1999; Webster et al., 1999; Krishnamurty and Kirtman, 2003; Meyers et al., 2007). In addition, the driving mechanisms of ENSO and IOD during the Holocene are not fully understood, even though linkages with insolation were reported (e.g., Otto-Bliesner et al., 2003; Liu et al., 2000; Timmermann et al., 2007; Zheng et al., 2008; Tudhope et al., 2001; Moy et al., 2002; Koutavas et al., 2006; Conroy et al., 2008; Kuhnert et al., 2014; Liu et al., 2003; Abram et al., 2007). The IOD signals in the tropical Indian Ocean may additionally be overridden by the global mean temperature (e.g., Vecchi and Soden, 2007; Zheng et al., 2013), or the signals could be strongly influenced by monsoonal changes in the surrounding landmasses (e.g., Abram et al., 2007; Qiu et al., 2012).

Despite the complicated relationships, it is possible that climate of NW Madagascar has been influenced by ITCZ, IOD, and ENSO, but this is still poorly understood during the Holocene. We are aware that the temporal and spatial resolution of available records make this investigation challenging, and we understand that the range of uncertainty of radiometric ages of several paleoclimate data could be another barrier to fully evaluate such relationship (see for example Fig. 7 of Kuhnert et al., 2014).

6. Conclusions

Petrography, mineralogy, and stable isotope records from Stalagmite ANJB-2, from Anjohibe Cave, and Stalagmite MAJ-5, from Anjokipoty Cave, combine to suggest three distinct intervals of changing climate in Madagascar during the Holocene: relatively wet conditions during the MEHI, relatively drier conditions, possibly due to episodic dryness, during the MMHI, and relatively wet conditions during the MLHI. The timing of stalagmite deposition during the MEHI and the MLHI in NW Madagascar could be attributed to a more southward migration and/or an expanded ITCZ, increasing the duration of the summer rainy seasons, perhaps linked to a stronger Malagasy monsoon. This could have been tied to insolation, the temperature gradient between the two hemispheres, and weakening of the AMOC. In contrast, the c. 6500 year depositional hiatus during the MMHI could indicate a northward migration of the ITCZ, leading to relatively drier conditions in NW Madagascar. The evidence of the 8.2 ka event in the Malagasy records further suggests a strong link between paleoenvironmental changes in Madagascar and abrupt climatic events in the NH, suggesting that during the MEHI Madagascar's climate was very sensitive to abrupt ocean-atmosphere events in the NH.

Although the ITCZ is one of the climatic drivers influencing climate in Madagascar and its surrounding locations, several climatic factors need to be investigated in more detail. For example, we do not fully understand if the latitudinal migration is paired with the expansion and/or expansion of the ITCZ, responsible to changes in several monsoon systems. In addition, the interplay between ITCZ and other factors involving changes in sea surface temperatures, particularly IOD-ENSO, needs to be investigated in details. Data-model comparison seems to be an approach to better understand such relationship. The lack of spatial and temporal resolution of paleoclimate records is still a challenge to fully understand the climate system during the Holocene.

Author Contribution

N.R.G.V. conceived the research and experiments. N.R.G.V, G.K, A.F.M.R, and M.O.M.R did the fieldwork and collected the samples. X.L., G.K., H.C., R.L.E, and N.R.G.V contributed to the ^{230}Th dating analyses. N.R.G.V provided detailed investigation of the two stalagmites, provided stable isotope measurements, prepared thin sections, and conducted X-ray diffraction analyses. G.K. also assisted with the isotopic measurements on Stalagmite ANJB-2. N.R.G.V. wrote the first draft of the manuscript and led the writing. L.B.R. and G.A.B. provided a thorough review of the draft. N.R.G.V. and L.B.R. discussed and revised the manuscript, with additional comments from L.W. N.R.G.V revised the paper with input from all authors, reviewers, and editors.

Competing Interests

The authors declare no conflict of interest.

Acknowledgments

This work was supported by grants from (1) the National Natural Science Foundation of China (NSFC 41230524, NBRP 2013CB955902, and NSFC 41472140) to Hai Cheng and Gayatri Kathayat, (2) the Geological Society of America Research Grant (GSA 11166-16) and John Montagne Fund Award to N. Voarintsoa, (3) the Miriam Watts-Wheeler Graduate Student Grant from the Department of Geology at UGA to N. Voarintsoa, and (4) the International Association of Sedimentology Post-Graduate Grant to N. Voarintsoa. We also thank the Schlumberger Foundation for providing additional support to N. Voarintsoa's research. We thank the Department of Geology at the University of Antananarivo, in Madagascar, the Ministry of Energy and Mines, the local village and guides in Majunga for easing our research in Madagascar. We specifically thank Prof. Voahangy Ratrimo, former Department Head of the Department of Geology at the University of Antananarivo, for collaborating with us and for giving us permission to conduct field expedition in Madagascar. We thank Prof. Paul Schroeder for giving us access to use the X-ray diffractometer of the Geology Department to conduct analysis on the mineralogy of the two stalagmites. We thank Prof. John Shields of the Georgia Electron Microscope, University of Georgia, for giving Voarintsoa access to use the Zeiss 1450EP (Carl Zeiss, Inc., Thornwood, NY) for SEM purposes. We also thank Prof. Sally Walker for allowing us to use the microscope of the paleontology lab and for helping us photograph the stalagmites at very high resolution. We also thank Prof. John Chiang of the University of California at Berkeley, for sharing his thoughts and guiding us to literature of relevance to this study.

References

Abram, N. J., Gagan, M. K., Liu, Z. Y., Hantoro, W. S., McCulloch, M. T., and Suwargadi, B. W.: Seasonal characteristics of the Indian Ocean Dipole during the Holocene epoch, Nature, 445, 299-302, Doi 10.1038/Nature05477, 2007.

Abram, N. J., McGregor, H. V., Gagan, M. K., Hantoro, W. S., and Suwargadi, B. W.: Oscillations in the southern extent of the Indo-Pacific Warm Pool during the mid-Holocene, Quaternary Sci Rev, 28, 2794-2803, Doi 10.1016/J.Quascirev.2009.07.006, 2009.

Abram, N. J., Gagan, M. K., Cole, J. E., Hantoro, W. S., and Mudelsee, M.: Recent intensification of tropical climate variability in the Indian Ocean, Nature Geosci, 1, 849-853, 2008.

Alley, R. B., Mayewski, P. A., Sowers, T., Stuiver, M., Taylor, K. C., and Clark, P. U.: Holocene climatic instability: A prominent, widespread event 8200 yr ago, Geology, 25, 483-486, 1997.

Asrat, A., Baker, A., Mohammed, M. U., Leng, M. J., Van Calsteren, P., and Smith, C.: A high-resolution multi-proxy stalagmite record from Mechara, Southeastern Ethiopia: palaeohydrological implications for speleothem palaeoclimate reconstruction, J Quaternary Sci, 22, 53-63, Doi 10.1002/Jqs.1013, 2007.

Barber, D. C., Dyke, A., Hillaire-Marcel, C., Jennings, A. E., Andrews, J. T., Kerwin, M. W., Bilodeau, G., McNeely, R., Southon, J., Morehead, M. D., and Gagnon, J. M.: Forcing of the cold event of 8,200 years ago by catastrophic drainage of Laurentide lakes, Nature, 400, 344-348, Doi 10.1038/22504, 1999.

Bard, E., Rostek, F., and Sonzogni, C.: Interhemispheric synchrony of the last deglaciation inferred from alkenone palaeothermometry, Nature, 385, 707-710, Doi 10.1038/385707a0, 1997.

Beal, L. M., De Ruijter, W. P. M., Biastoch, A., Zahn, R., and 136, S. W. I. W. G.: On the role of the Agulhas system in ocean circulation and climate, Nature, 472, 429-436, Doi 10.1038/Nature09983, 2011.

Behera, S. K., Krishnan, R., and Yamagata, T.: Unusual ocean-atmosphere conditions in the tropical Indian Ocean during 1994, Geophys Res Lett, 26, 3001-3004, Doi 10.1029/1999gl010434, 1999.

Behera, S., Brandt, P., and Reverdin, G.: The Tropical Ocean Circulation and Dynamics, in: Ocean Circulation and Climate: A 21st Century Perspective, edited by: Siedler, G., Griffies, S., Gould, J., and Church, J., Elsevier, Amsterdam, Netherlands, 385-412, 2013.

Berger, A., and Loutre, M. F.: Insolation Values for the Climate of the Last 10 million years, Quaternary Sci Rev, 10, 297-317, Doi 10.1016/0277-3791(91)90033-Q, 1991.

Black, E., Slingo, J., and Sperber, K. R.: An observational study of the relationship between excessively strong short rains in coastal East Africa and Indian Ocean SST, Mon Weather Rev, 131, 74-94, Doi 10.1175/1520-0493(2003)131<0074:Aosotr>2.0.Co;2, 2003.

Bond, G., Kromer, B., Beer, J., Muscheler, R., Evans, M. N., Showers, W., Hoffmann, S., Lotti-Bond, R., Hajdas, I., and Bonani, G.: Persistent solar influence on north Atlantic climate during the Holocene, Science, 294, 2130-2136, Doi 10.1126/Science.1065680, 2001.

Bond, G., Showers, W., Cheseby, M., Lotti, R., Almasi, P., deMenocal, P., Priore, P., Cullen, H., Hajdas, I., and Bonani, G.: A pervasive millennial-scale cycle in North Atlantic Holocene and glacial climates, Science, 278, 1257-1266, DOI 10.1126/science.278.5341.1257, 1997.

Bosák, P.: Dating of processes in karst and caves: implication for show caves presentation, 6th ISCA Congress Proceedings, Slovakia, 2011, 34-41, 2011.

Braconnot, P., Marti, O., Joussaume, S., and Leclainche, Y.: Ocean feedback in response to 6 kyr BP insolation, J Climate, 13, 1537-1553, 2000.

Braconnot, P., Otto-Bliesner, B., Harrison, S., Joussaume, S., Peterchmitt, J. Y., Abe-Ouchi, A., Crucifix, M., Driesschaert, E., Fichefet, T., Hewitt, C. D., Kageyama, M., Kitoh, A., Laine, A., Loutre, M. F., Marti, O., Merkel, U., Ramstein, G., Valdes, P., Weber, S. L., Yu, Y., and Zhao, Y.: Results of PMIP2 coupled simulations of the Mid-Holocene and Last Glacial Maximum - Part 1: experiments and large-scale features, Clim Past, 3, 261-277, 2007.

Broccoli, A. J., Dahl, K. A., and Stouffer, R. J.: Response of the ITCZ to Northern Hemisphere cooling, Geophys Res Lett, 33, 10.1029/2005gl024546, 2006.

Broecker, W. S.: Paleocean circulation during the Last Deglaciation: A bipolar seesaw?, Paleoceanography, 13, 119-121, 10.1029/97PA03707, 1998.

Brook, G. A., Rafter, M. A., Railsback, L. B., Sheen, S. W., and Lundberg, J.: A high-resolution proxy record of rainfall and ENSO since AD 1550 from layering in stalagmites from Anjohibe Cave, Madagascar, Holocene, 9, 695-705, Doi 10.1191/095968399677907790, 1999.

Brown, J., Lynch, A. H., and Marshall, A. G.: Variability of the Indian Ocean Dipole in coupled model paleoclimate simulations, J Geophys Res-Atmos, 114, 10.1029/2008jd010346, 2009.

Büntgen, U., Tegel, W., Nicolussi, K., McCormick, M., Frank, D., Trouet, V., Kaplan, J. O., Herzig, F., Heussner, K. U., Wanner, H., Luterbacher, J., and Esper, J.: 2500 Years of European Climate Variability and Human Susceptibility, Science, 331, 578-582, DOI 10.1126/science.1197175, 2011.

Burney, D. A., Burney, L. P., Godfrey, L. R., Jungers, W. L., Goodman, S. M., Wright, H. T., and Jull, A. J. T.: A chronology for late prehistoric Madagascar, Journal of Human Evolution, 47, 25-63, Doi 10.1016/J.Jhevol.2004.05.005, 2004.

Burney, D. A., James, H. F., Grady, F. V., Rafamantanantsoa, J. G., Ramilisonina, Wright, H. T., and Cowart, J. B.: Environmental change, extinction and human activity: evidence from caves in NW Madagascar, Journal of Biogeography, 24, 755-767, 10.1046/J.1365-2699.1997.00146.X, 1997.

Burney, D. A., Robinson, G. S., and Burney, L. P.: Sporormiella and the late Holocene extinctions in Madagascar, P Natl Acad Sci USA, 100, 10800-10805, Doi 10.1073/Pnas.1534700100, 2003.

Burney, D. A.: Late Holocene Environmental-Changes in Arid Southwestern Madagascar, Quaternary Res, 40, 98-106, Doi 10.1006/Qres.1993.1060, 1993.

Burney, D. A.: Late Holocene Vegetational Change in Central Madagascar, Quaternary Res, 28, 130-143, Doi 10.1016/0033-5894(87)90038-X, 1987a.

Burney, D. A.: Late Quaternary Stratigraphic Charcoal Records from Madagascar, Quaternary Res, 28, 274-280, Doi 10.1016/0033-5894(87)90065-2, 1987b.

Burney, D. A.: Tropical islands as paleoecological laboratories: Gauging the consequences of human arrival, Hum Ecol, 25, 437-457, Doi 10.1023/A:1021823610090, 1997.

Burns, S. J., Godfrey, L. R., Faina, P., McGee, D., Hardt, B., Ranivoharimanana, L., and Randrianasy, J.: Rapid human-induced landscape transformation in Madagascar at the end of the first millennium of the Common Era, Quaternary Sci Rev, 134, 92-99, 10.1016/j.quascirev.2016.01.007, 2016.

Cabrol, P., and Coudray, J.: Climatic fluctuations influence the genesis and diagenesis of carbonate speleothems in southwestern France, National Speleological Society Bulletin 44, 112-117, 1982.

Carlson, A. E., Legrande, A. N., Oppo, D. W., Came, R. E., Schmidt, G. A., Anslow, F. S., Licciardi, J. M., and Obbink, E. A.: Rapid early Holocene deglaciation of the Laurentide ice sheet, Nat Geosci, 1, 620-624, 10.1038/ngeo285, 2008.

Cheng, H., Edwards, R. L., Shen, C. C., Polyak, V. J., Asmerom, Y., Woodhead, J., Hellstrom, J., Wang, Y. J., Kong, X. G., Spotl, C., Wang, X. F., and Alexander, E. C.: Improvements in Th-230 dating, Th-230 and U-234 half-life values, and U-Th isotopic measurements by multi-collector inductively coupled plasma mass spectrometry, Earth Planet Sc Lett, 371, 82-91, Doi 10.1016/J.Epsl.2013.04.006, 2013.

Cheng, H., Fleitmann, D., Edwards, R. L., Wang, X. F., Cruz, F. W., Auler, A. S., Mangini, A., Wang, Y. J., Kong, X. G., Burns, S. J., and Matter, A.: Timing and structure of the 8.2 kyr BP event inferred from delta O-18 records of stalagmites from China, Oman, and Brazil, Geology, 37, 1007-1010, Doi 10.1130/G30126a.1, 2009.

Chiang, J. C. H., and Bitz, C. M.: Influence of high latitude ice cover on the marine Intertropical Convergence Zone, Clim Dynam, 25, 477-496, 10.1007/s00382-005-0040-5, 2005.

Chiang, J. C. H., and Friedman, A. R.: Extratropical Cooling, Interhemispheric Thermal Gradients, and Tropical Climate Change, Annual Review of Earth and Planetary Sciences, 40, 383-412, 10.1146/Annurev-Earth-042711-105545, 2012.

Chiang, J. C. H.: The Tropics in Paleoclimate, Annual Review of Earth and Planetary Sciences, 37, 263-297, 10.1146/annurev.earth.031208.100217, 2009.

Clark, P. U., Marshall, S. J., Clarke, G. K. C., Hostetler, S. W., Licciardi, J. M., and Teller, J. T.: Freshwater Forcing of Abrupt Climate Change During the Last Glaciation, Science, 293, 283-287, 10.1126/science.1062517, 2001.

Conroy, J. L., Overpeck, J. T., Cole, J. E., Shanahan, T. M., and Steinitz-Kannan, M.: Holocene changes in eastern tropical Pacific climate inferred from a Galápagos lake sediment record, Quaternary Sci Rev, 27, 1166-1180, 2008.

Crowley, B. E., and Samonds, K. E.: Stable carbon isotope values confirm a recent increase in grasslands in northwestern Madagascar, The Holocene, 23, 1066-1073, Doi 10.1177/0959683613484675, 2013.

Crowley, B. E.: A refined chronology of prehistoric Madagascar and the demise of the megafauna, Quaternary Sci Rev, 29, 2591-2603, Doi 10.1016/J.Quascirev.2010.06.030, 2010.

Crowley, T. J.: North Atlantic Deep Water cools the southern hemisphere, Paleoceanography, 7, 489-497, 10.1029/92PA01058, 1992.

Crowther, A., Lucas, L., Helm, R., Horton, M., Shipton, C., Wright, H. T., Walshaw, S., Pawlowicz, M., Radimilahy, C., Douka, K., Picornell-Gelabert, L., Fuller, D. Q., and Boivin, N. L.: Ancient crops provide first archaeological signature of the westward Austronesian expansion, P Natl Acad Sci USA, 113, 6635-6640, 10.1073/pnas.1522714113, 2016.

Cruz, F. W., Burns, S. J., Karmann, I., Sharp, W. D., Vuille, M., Cardoso, A. O., Ferrari, J. A., Dias, P. L. S., and Viana, O.: Insolation-driven changes in atmospheric circulation over the past 116,000 years in subtropical Brazil, Nature, 434, 63-66, Doi 10.1038/Nature03365., 2005.

Dahl, K., Broccoli, A., and Stouffer, R.: Assessing the role of North Atlantic freshwater forcing in millennial scale climate variability: a tropical Atlantic perspective, Clim Dynam, 24, 325-346, 10.1007/s00382-004-0499-5, 2005.

Daley, T. J., Thomas, E. R., Holmes, J. A., Street-Perrott, F. A., Chapman, M. R., Tindall, J. C., Valdes, P. J., Loader, N. J., Marshall, J. D., Wolff, E. W., Hopley, P. J., Atkinson, T., Barber, K. E., Fisher, E. H., Robertson, I., Hughes, P. D. M., and Roberts, C. N.: The 8200yr BP cold event in stable isotope records from the North Atlantic region, Global Planet Change, 79, 2011.

Dewar, R. E., and Richard, A. F.: Evolution in the hypervariable environment of Madagascar, P Natl Acad Sci USA, 104, 13723-13727, 10.1073/pnas.0704346104, 2007.

DGM [Direction Générale de la Météorologie]: Le changement climatique à Madagascar. 2008.

Dong, B. W., and Sutton, R. T.: Adjustment of the coupled ocean-atmosphere system to a sudden change in the Thermohaline Circulation, Geophys Res Lett, 29, 2002.

Dong, B., and Sutton, R. T.: Enhancement of ENSO variability by a weakened Atlantic thermohaline circulation in a coupled GCM, J Climate, 20, 4920-4939, 10.1175/Jcli4284.1, 2007.

Dong, J. G., Wang, Y. J., Cheng, H., Hardt, B., Edwards, R. L., Kong, X. G., Wu, J. Y., Chen, S. T., Liu, D. B., Jiang, X. Y., and Zhao, K.: A high-resolution stalagmite record of the Holocene East Asian monsoon from Mt Shennongjia, central China, Holocene, 20, 257-264, Doi 10.1177/0959683609350393, 2010.

Dorale, J. A., Edwards, R. L., Alexander, E. C., Shen, C.-C., Richards, D. A., and Cheng, H.: Uranium-Series Dating of Speleothems: Current Techniques, Limits, & Applications, in: Studies of Cave Sediments: Physical and Chemical Records of Paleoclimate, edited by: Sasowsky, I. D., and Mylroie, J., Springer US, Boston, MA, 177-197, 2004.

Douglass, K., and Zinke, J.: Forging Ahead By Land and By Sea: Archaeology and Paleoclimate Reconstruction in Madagascar, Afr Archaeol Rev, 32, 267-299, 10.1007/s10437-015-9188-5, 2015.

Dutton, A., Bard, E., Antonioli, F., Esat, T. M., Lambeck, K., and McCulloch, M. T.: Phasing and amplitude of sea-level and climate change during the penultimate interglacial, Nat Geosci, 2, 355-359, 10.1038/Ngeo470, 2009.

Dykoski, C. A., Edwards, R. L., Cheng, H., Yuan, D. X., Cai, Y. J., Zhang, M. L., Lin, Y. S., Qing, J. M., An, Z. S., and Revenaugh, J.: A high-resolution, absolute-dated Holocene and deglacial Asian monsoon record from Dongge Cave, China, Earth Planet Sc Lett, 233, 71-86, 10.1016/j.epsl.2005.01.036, 2005.

Edwards, R. L., Chen, J. H., and Wasserburg, G. J.: U-238 U-234-Th-230-Th-232 Systematics and the Precise Measurement of Time over the Past 500000 Years, Earth Planet Sc Lett, 81, 175-192, 1987.

Fairchild, I. J., and Baker, A.: Speleothem Science: From Processes to Past Environments, edited by: Bradley, R., Wiley-Blackwell, 2012.

Fairchild, I. J., and McMillan, E. A.: Speleothems as indicators of wet and dry periods, International Journal of Speleology, 36, 69-74, 2007.

Fairchild, I. J., Borsato, A., Tooth, A. F., Frisia, S., Hawkesworth, C. J., Huang, Y. M., McDermott, F., and Spiro, B.: Controls on trace element (Sr-Mg) compositions of carbonate cave waters: implications for speleothem climatic records, Chem Geol, 166, 255-269, Doi 10.1016/S0009-2541(99)00216-8, 2000.

Fleitmann, D., Burns, S. J., Mangini, A., Mudelsee, M., Kramers, J., Villa, I., Neff, U., Al-Subbary, A. A., Buettner, A., Hippler, D., and Matter, A.: Holocene ITCZ and Indian monsoon dynamics recorded in stalagmites from Oman and Yemen (Socotra), Quaternary Sci Rev, 26, 170-188, 10.1016/J.Quascirev.2006.04.012, 2007.

Fleitmann, D., Burns, S. J., Mudelsee, M., Neff, U., Kramers, J., Mangini, A., and Matter, A.: Holocene forcing of the Indian monsoon recorded in a stalagmite from Southern Oman, Science, 300, 1737-1739, Doi 10.1126/Science.1083130, 2003.

Frierson, D. M. W., and Hwang, Y. T.: Extratropical Influence on ITCZ Shifts in Slab Ocean Simulations of Global Warming, J Climate, 25, 720-733, 10.1175/Jcli-D-11-00116.1, 2012.

Frisia, S., Borsato, A., Fairchild, I. J., McDermott, F., and Selmo, E. M.: Aragonite–calcite relationships in speleothems (Grotte de Clamouse, France): environment, fabrics, and carbonate geochemistry., J Sediment Res, 772, 687-699, 2002.

Garcin, Y., Vincens, A., Williamson, D., Guiot, J., and Buchet, G.: Wet phases in tropical southern Africa during the last glacial period, Geophys Res Lett, 33, 10.1029/2005GL025531, 2006.

Gasse, F., and Van Campo, E.: A 40,000-yr pollen and diatom record from Lake Tritrivakely, Madagascar, in the southern tropics, Quaternary Res, 49, 299-311, Doi 10.1006/Qres.1998.1967, 1998.

Gasse, F.: Hydrological changes in the African tropics since the Last Glacial Maximum, Quaternary Sci Rev, 19, 189-211, Doi 10.1016/S0277-3791(99)00061-X, 2000.

Gommery, D., Ramanivosoa, B., Faure, M., Guerin, C., Kerloc'h, P., Senegas, F., and Randrianantenaina, H.: Oldest evidence of human activities in Madagascar on subfossil hippopotamus bones from Anjohibe (Mahajanga Province), Cr Palevol, 10, 271-278, 10.1016/j.crpv.2011.01.006, 2011.

Guan, Z. Y., and Yamagata, T.: The unusual summer of 1994 in East Asia: IOD teleconnections, Geophys Res Lett, 30, Artn 1544 10.1029/2002gl016831, 2003.

Haug, G. H., Hughen, K. A., Sigman, D. M., Peterson, L. C., and Rohl, U.: Southward migration of the intertropical convergence zone through the Holocene, Science, 293, 1304-1308, Doi 10.1126/Science.1059725, 2001.

Head, M. J., and Gibbard, P. L.: Formal subdivision of the Quaternary System/Period: Past, present, and future, Quatern Int, 383, 4-35, 10.1016/j.quaint.2015.06.039, 2015.

Holmgren, K., Karlen, W., and Shaw, P. A.: Paleoclimatic Significance of the Stable Isotopic Composition and Petrology of a Late Pleistocene Stalagmite from Botswana, Quaternary Res, 43, 320-328, DOI 10.1006/qres.1995.1038, 1995.

Holmgren, K., Lee-Thorp, J. A., Cooper, G. R. J., Lundblad, K., Partridge, T. C., Scott, L., Sithaldeen, R., Talma, A. S., and Tyson, P. D.: Persistent millennial-scale climatic variability over the past 25,000 years in Southern Africa, Quaternary Sci Rev, 22, 2311-2326, 10.1016/S0277-3791(03)00204-X, 2003.

Holzhauser, H., Magny, M., and Zumbuhl, H. J.: Glacier and lake-level variations in west-central Europe over the last 3500 years, Holocene, 15, 789-801, 10.1191/0959683605hl853ra, 2005.

Johnson, K. R., Hu, C. Y., Belshaw, N. S., and Henderson, G. M.: Seasonal trace-element and stable-isotope variations in a Chinese speleothem: The potential for high-resolution paleomonsoon reconstruction, Earth Planet Sc Lett, 244, 394-407, 10.1016/j.epsl.2006.01.064, 2006.

Jungers, W. L., Demes, B., and Godfrey, L. R.: How big were the "Giant" extinct lemurs of Madagascar?, in: Elwyn Simons: A search for origins, edited by: Fleagle, J. G., and Gilbert, C. G., Springer, New York, 343-360, 2008.

Jury, M. R.: The Climate of Madagascar, in: The Natural History of Madagascar, edited by: Goodman, S. M., and Benstead, J. P., Chicago: Universtity of Chicago, 75-87, 2003.

Kang, S. M., Held, I. M., Frierson, D. M. W., and Zhao, M.: The response of the ITCZ to extratropical thermal forcing: Idealized slab-ocean experiments with a GCM, J Climate, 21, 3521-3532, 10.1175/2007jcli2146.1, 2008.

Karmann, I., Cruz, F. W., Viana, O., and Burns, S. J.: Climate influence on geochemistry parameters of waters from Santana-Perolas cave system, Brazil, Chem Geol, 244, 232-247, 10.1016/j.chemgeo.2007.06.029, 2007.

Kim, S. T., O'Neil, J. R., Hillaire-Marcel, C., and Mucci, A.: Oxygen isotope fractionation between synthetic aragonite and water: Influence of temperature and Mg2+ concentration, Geochim Cosmochim Ac, 71, 4704-4715, 10.1016/J.Gca.2007.04.019, 2007.

Kim, S.-T., and O'Neil, J. R.: Equilibrium and nonequilibrium oxygen isotope effects in synthetic carbonates, Geochim Cosmochim Ac, 61, 3461-3475, doi.org/10.1016/S0016-7037(97)00169-5, 1997.

Kleiven, H. F., Kissel, C., Laj, C., Ninnemann, U. S., Richter, T. O., and Cortijo, E.: Reduced North Atlantic Deep Water coeval with the glacial Lake Agassiz freshwater outburst, Science, 319, 60-64, 10.1126/science.1148924, 2008.

Konecky, B. L., Russell, J. M., Johnson, T. C., Brown, E. T., Berke, M. A., Werne, J. P., and Huang, Y. S.: Atmospheric circulation patterns during late Pleistocene climate changes at Lake Malawi, Africa, Earth Planet Sc Lett, 312, 318-326, 10.1016/j.epsl.2011.10.020, 2011.

Koutavas, A., deMenocal, P. B., Olive, G. C., and Lynch-Stieglitz, J.: Mid-Holocene El Niño–Southern Oscillation (ENSO) attenuation revealed by individual foraminifera in eastern tropical Pacific sediments, Geology, 34, 993-996, 10.1130/G22810A.1, 2006.

Krishnamurthy, V., and Kirtman, B. P.: Variability of the Indian Ocean: Relation to monsoon and ENSO, Q J Roy Meteor Soc, 129, 1623-1646, 10.1256/qj.01.166, 2003.

Kuhnert, H., Kuhlmann, H., Mohtadi, M., Meggers, H., Baumann, K. H., and Patzold, J.: Holocene tropical western Indian Ocean sea surface temperatures in covariation with climatic changes in the Indonesian region, Paleoceanography, 29, 423-437, 10.1002/2013pa002555, 2014.

Kutzbach, J. E., and Liu, Z.: Response of the African Monsoon to Orbital Forcing and Ocean Feedbacks in the Middle Holocene, Science, 278, 440, 1997.

Lachniet, M. S., Bernal, J. P., Asmerom, Y., and Polyak, V.: Uranium loss and aragonite-calcite age discordance in a calcitized aragonite stalagmite, Quat Geochronol, 14, 26-37, 10.1016/j.quageo.2012.08.003, 2012.

Lambert, W. J., and Aharon, P.: Controls on dissolved inorganic carbon and delta C-13 in cave waters from DeSoto Caverns: Implications for speleothem delta C-13 assessments, Geochim Cosmochim Ac, 75, 753-768, 10.1016/j.gca.2010.11.006, 2011.

Lee, T., and McPhaden, M. J.: Decadal phase change in large-scale sea level and winds in the Indo-Pacific region at the end of the 20th century, Geophys Res Lett, 35, 10.1029/2007gl032419, 2008.

Li, T., Wang, B., Chang, C. P., and Zhang, Y. S.: A theory for the Indian Ocean dipole-zonal mode, J Atmos Sci, 60, 2119-2135, 10.1175/1520-0469(2003)060<2119:Atftio>2.0.Co;2, 2003.

Liang, F., Brook, G. A., Kotlia, B. S., Railsback, L. B., Hardt, B., Cheng, H., Edwards, R. L., and Kandasamy, S.: Panigarh cave stalagmite evidence of climate change in the Indian Central Himalaya since AD 1256: Monsoon breaks and winter southern jet depressions, Quaternary Sci Rev, 124, 145-161, 2015.

Lindesay, J. A.: Past Climates of Southern Africa, in: Climates of the Southern Continents: Present, Past and Future, edited by: Hobbs, J. E., Lindesay, J. A., and Bridgman, H. A., John Wiley & Sons Ltd., England, 161-206, 1998.

Liu, Z., Kutzbach, J., and Wu, L.: Modeling climate shift of El Nino variability in the Holocene, Geophys Res Lett, 27, 2265-2268, 10.1029/2000GL011452, 2000.

Liu, Y. H., Henderson, G. M., Hu, C. Y., Mason, A. J., Charnley, N., Johnson, K. R., and Xie, S. C.: Links between the East Asian monsoon and North Atlantic climate during the 8,200 year event, Nat Geosci, 6, 117-120, 10.1038/Ngeo1708, 2013.

Ljungqvist, F. C.: The Spatio-Temporal Pattern of the Mid-Holocene Thermal Maximum, Geografie-Prague, 116, 91-110, 2011.

Lutjeharms, J. R. E.: The Aghulas Current, Springer, 2006.

MacPhee, R. D. E., and Burney, D. A.: Dating of Modified Femora of Extinct Dwarf Hippopotamus from Southern Madagascar - Implications for Constraining Human Colonization and Vertebrate Extinction Events, J Archaeol Sci, 18, 695-706, Doi 10.1016/0305-4403(91)90030-S, 1991.

Mann, M. E., Bradley, R. S., and Hughes, M. K.: Northern hemisphere temperatures during the past millennium: Inferences, uncertainties, and limitations, Geophys Res Lett, 26, 759-762, 10.1029/1999GL900070, 1999.

Mann, M. E., Bradley, R. S., and Hughes, M. K.: Global-scale temperature patterns and climate forcing over the past six centuries, Nature, 392, 779-787, 1998.

Marcott, S. A., Shakun, J. D., Clark, P. U., and Mix, A. C.: A Reconstruction of Regional and Global Temperature for the Past 11,300 Years, Science, 339, 1198, 2013.

Matsumoto, K., and Burney, D. A.: Late Holocene environments at Lake Mitsinjo, northwestern Madagascar, The Holocene, 4, 16-24, 1994.

Mayewski, P. A., Rohling, E. E., Stager, J. C., Karlen, W., Maasch, K. A., Meeker, L. D., Meyerson, E. A., Gasse, F., van Kreveld, S., Holmgren, K., Lee-Thorp, J., Rosqvist, G., Rack, F., Staubwasser, M., Schneider, R. R., and Steig, E. J.: Holocene climate variability, Quaternary Res, 62, 243-255, Doi 10.1016/J.Yqres.2004.07.001, 2004.

McDonald, J., Drysdale, R., Hill, D., Chisari, R., and Wong, H.: The hydrochemical response of cave drip waters to sub-annual and inter-annual climate variability, Wombeyan Caves, SE Australia, Chem Geol, 244, 605-623, 2007.

McGee, D., Donohoe, A., Marshall, J., and Ferreira, D.: Changes in ITCZ location and cross-equatorial heat transport at the Last Glacial Maximum, Heinrich Stadial 1, and the mid-Holocene, Earth Planet Sc Lett, 390, 69-79, 10.1016/J.Epsl.2013.12.043, 2014.

McMillan, E. A., Fairchild, I. J., Frisia, S., Borsato, A., and McDermott, F.: Annual trace element cycles in calcite-aragonite speleothems: evidence of drought in the western Mediterranean 1200-1100 yr BP, J Quaternary Sci, 20, 423-433, 10.1002/jqs.943, 2005.

Meyers, G., McIntosh, P., Pigot, L., and Pook, M.: The Years of El Niño, La Niña, and Interactions with the Tropical Indian Ocean, J Climate, 20, 2872-2880, 10.1175/JCLI4152.1, 2007.

Middleton, J., and Middleton, V.: Karst and caves of Madagascar, Cave and Karst Science, 29, 13-20, 2002.

Moy, C. M., Seltzer, G. O., Rodbell, D. T., and Anderson, D. M.: Variability of El Nino/Southern Oscillation activity at millennial timescales during the Holocene epoch, Nature, 420, 162-165, 2002.

Murray, J. W.: The deposition of calcite and aragonite in caves., J Geol, 62, 481-492, 1954.

Nassor, A., and Jury, M. R.: Intra-seasonal climate variability of Madagascar. Part 1: Mean summer conditions, Meteorol Atmos Phys, 65, 31-41, Doi 10.1007/Bf01030267, 1998.

Nicholson, S.E.: Environmental change within the historical period, in: The Physical Geography of Africa, Goudie, A.S., Adams, W.M., Orme, A. (Eds.), Oxford University Press, Oxford, 60–75, 1996.

Niggemann, S., Mangini, A., Mudelsee, M., Richter, D. K., and Wurth, G.: Sub-Milankovitch climatic cycles in Holocene stalagmites from Sauerland, Germany, Earth Planet Sc Lett, 216, 539-547, Doi 10.1016/S0012-821x(03)00513-2, 2003.

Otto-Bliesner, B. L., Brady, E. C., Shin, S.-I., Liu, Z., and Shields, C.: Modeling El Niño and its tropical teleconnections during the last glacial-interglacial cycle, Geophys Res Lett, 30, n/a-n/a, 10.1029/2003GL018553, 2003.

Partridge, T. C., Demenocal, P. B., Lorentz, S. A., Paiker, M. J., and Vogel, J. C.: Orbital forcing of climate over South Africa: A 200,000-year rainfall record from the Pretoria saltpan, Quaternary Sci Rev, 16, 1125-1133, 1997.

Paul, D., and Skrzypek, G.: Assessment of carbonate-phosphoric acid analytical technique performed using GasBench II in continuous flow isotope ratio mass spectrometry, Int J Mass Spectrom, 262, 180-186, 10.1016/j.ijms.2006.11.006, 2007.

Perrin, C., Prestimonaco, L., Servelle, G., Tilhac, R., Maury, M., and Cabrol, P.: Aragonite–calcite speleothems: identifying original and diagenetic features, J Sediment Res, 84, 245-269, 2014.

Pobeguin, T.: Sur les concrétions calcaires observés dans la Grotte de Moulis (Ariège), Société Géologique de la France, Compte Rendus, 241, 1791-1793, 1965.

Qiu, Y., Cai, W., Li, L., and Guo, X.: Argo profiles variability of barrier layer in the tropical Indian Ocean and its relationship with the Indian Ocean Dipole, Geophys Res Lett, 39, n/a-n/a, 10.1029/2012GL051441, 2012.

Railsback, L. B., Akers, P. D., Wang, L. X., Holdridge, G. A., and Voarintsoa, N. R.: Layer-bounding surfaces in stalagmites as keys to better paleoclimatological histories and chronologies, International Journal of Speleology, 42, 167-180, 10.5038/1827-806x.42.3.1, 2013.

Railsback, L. B., Brook, G. A., Chen, J., Kalin, R., and Fleisher, C. J.: Environmental Controls on the Petrology of a Late Holocene Speleothem from Botswana with annual layers of aragonite and calcite, J Sediment Res A, 64, 147-155, 1994.

Railsback, L. B., Brook, G. A., Ellwood, B. B., Liang, F., Cheng, H., and Edwards, R. L.: A record of wet glacial stages and dry interglacial stages over the last 560kyr from a standing massive stalagmite in Carlsbad Cavern, New Mexico, USA, Palaeogeography, Palaeoclimatology, Palaeoecology, 438, 256-266, http://dx.doi.org/10.1016/j.palaeo.2015.08.010, 2015.

Railsback, L. B., Brook, G. A., Liang, F., Marais, E., Cheng, H., and Edwards, R. L.: A multi-proxy stalagmite record from northwestern Namibia of regional drying with increasing global-scale warmth over the last 47kyr: The interplay of a globally shifting ITCZ with regional currents, winds, and rainfall, Palaeogeography, Palaeoclimatology, Palaeoecology, 461, 109-121, 2016.

Railsback, L. B., Xiao, H. L., Liang, F. Y., Akers, P. D., Brook, G. A., Dennis, W. M., Lanier, T. E., Tan, M., Cheng, H., and Edwards, R. L.: A stalagmite record of abrupt climate change and possible Westerlies-derived atmospheric precipitation during the Penultimate Glacial Maximum in northern China, Palaeogeogr Palaeocl, 393, 30-44, Doi 10.1016/J.Palaeo.2013.10.013, 2014.

Railsback, L.B.: Atlas of speleothem microfabrics.Available at. www.gly.uga.edu/ railsback/speleoatlas/SAindex1.html, 2000.

Renssen, H., Goosse, H., Fichefet, T., and Campin, J. M.: The 8.2 kyr BP event simulated by a Global Atmosphere—Sea-Ice—Ocean Model, Geophys Res Lett, 28, 1567-1570, 10.1029/2000GL012602, 2001.

Renssen, H., Goosse, H., Crosta, X., and Roche, D. M.: Early Holocene Laurentide Ice Sheet deglaciation causes cooling in the high-latitude Southern Hemisphere through oceanic teleconnection, Paleoceanography, 25, PA3204, doi10.1029/2009pa001854, 2010.

Romanek, C. S., Grossman, E. L., and Morse, J. W.: Carbon Isotopic Fractionation in Synthetic Aragonite and Calcite - Effects of Temperature and Precipitation Rate, Geochim Cosmochim Ac, 56, 419-430, Doi 10.1016/0016-7037(92)90142-6, 1992.

Rubinson, M., and Clayton, R. N.: Carbon-13 fractionation between aragonite and calcite, Geochim Cosmochim Ac, 33, 997-1002, 1969.

Sachs, J. P., Sachse, D., Smittenberg, R. H., Zhang, Z., Battisti, D. S., and Golubic, S.: Southward movement of the Pacific intertropical convergence zone AD[thinsp]1400-1850, Nature Geosci, 2, 519-525, 2009.

Saint-Ours, J. D.: Les phénomènes karstiques à Madagascar, Annales de Spéléologie, 14, 275-291, 1959.

Saji, N. H., and Yamagata, T.: Possible impacts of Indian Ocean Dipole mode events on global climate, Clim Res, 25, 151-169, Doi 10.3354/Cr025151, 2003.

Saji, N. H., Goswami, B. N., Vinayachandran, P. N., and Yamagata, T.: A dipole mode in the tropical Indian Ocean, Nature, 401, 360-363, 10.1038/43855, 1999.

Schefuß , E., Kuhlmann, H., Mollenhauer, G., Prange, M., and Patzold, J.: Forcing of wet phases in southeast Africa over the past 17,000 years, Nature, 480, 509-512, DOI 10.1038/nature10685, 2011.

Schefuß, E., Schouten, S., and Schneider, R. R.: Climatic controls on central African hydrology during the past 20,000[thinsp]years, Nature, 437, 1003-1006, 2005.

Schneider, T., Bischoff, T., and Haug, G. H.: Migrations and dynamics of the intertropical convergence zone, Nature, 513, 45-53, 10.1038/Nature13636, 2014.

Scholz, D., Tolzmann, J., Hoffmann, D. L., Jochum, K. P., Spötl, C., and Riechelmann, D. F. C.: Diagenesis of speleothems and its effect on the accuracy of 230Th/U-ages, Chem Geol, 387, 74-86, 2014.

Scholz, D., and Hoffmann, D. L.: StalAge - An algorithm designed for construction of speleothem age models, Quat Geochronol, 6, 369-382, 10.1016/j.quageo.2011.02.002, 2011.

Scholz, D., Hoffmann, D. L., Hellstrom, J., and Ramsey, C. B.: A comparison of different methods for speleothem age modelling, Quat Geochronol, 14, 94-104, 10.1016/j.quageo.2012.03.015, 2012.

Schott, F. A., Xie, S. P., and McCreary, J. P.: Indian Ocean Circulation and Climate Variability, Rev Geophys, 47, 10.1029/2007rg000245, 2009.

Scott, L.: Vegetation history and climate in the Savanna biome South Africa since 190,000 ka: a comparison of pollen data from the Tswaing Crater (the Pretoria Saltpan) and Wonderkrater, Quatern Int, 57, 215-223, 1999.

Scott, L., Thackeray, J.F.: Multivariate analysis of Late Pleistocene and Holocene pollen spectra from Wonderkrater, Transvaal, South Africa. S Afr J Sci, 83, 93–98. 1987.

Scroxton, N., Burns, S. J., McGee, D., Hardt, B., Godfrey, L. R., Ranivoharimanana, L., and Faina, P.: Hemispherically in-phase precipitation variability over the last 1700 years in a Madagascar speleothem record, Quaternary Sci Rev, 164, 25-36, 10.1016/j.quascirev.2017.03.017, 2017.

Seltzer, G., Rodbell, D., and Burns, S. J.: Isotopic evidence for Late Glacial and Holocene hydrologic change in tropical South America. Geology, 28, 35-38, 2000.

Shen, C.-C., Lawrence Edwards, R., Cheng, H., Dorale, J. A., Thomas, R. B., Bradley Moran, S., Weinstein, S. E., and Edmonds, H. N.: Uranium and thorium isotopic and concentration measurements by magnetic sector inductively coupled plasma mass spectrometry, Chem Geol, 185, 165-178, 2002.

Shinoda, T., Alexander, M. A., and Hendon, H. H.: Remote Response of the Indian Ocean to Interannual SST Variations in the Tropical Pacific, J Climate, 17, 362-372, 10.1175/1520-0442(2004)017<0362:RROTIO>2.0.CO;2, 2004.

Shtober-Zisu, N., Schwarcz, H. P., Konyer, N., Chow, T., and Noseworthy, M. D.: Macroholes in stalagmites and the search for lost water, J Geophys Res-Earth, 117, F03020, Doi 10.1029/2011jf002288, 2012.

Siegel, F. R.: Aspects of calcium carbonate deposition in Great Onyx Cave, Kentucky, Sedimentology, 4, 285–299, 1965.

Singarayer, J. S., and Burrough, S. L.: Interhemispheric dynamics of the African rainbelt during the late Quaternary, Quaternary Sci Rev, 124, 48-67, 2015.

Skrzypek, G., and Paul, D.: Delta C-13 analyses of calcium carbonate: comparison between the GasBench and elemental analyzer techniques, Rapid Commun Mass Sp, 20, 2915-2920, 10.1002/rcm.2688, 2006.

Sletten, H. R., Railsback, L. B., Liang, F. Y., Brook, G. A., Marais, E., Hardt, B. F., Cheng, H., and Edwards, R. L.: A petrographic and geochemical record of climate change over the last 4600 years from a northern Namibia stalagmite, with evidence of abruptly wetter climate at the beginning of southern Africa's Iron Age, Palaeogeogr Palaeocl, 376, 149-162, Doi 10.1016/J.Palaeo.2013.02.030, 2013.

Sonzogni, C., Bard, E., and Rostek, F.: Tropical sea-surface temperatures during the last glacial period: a view based on alkenones in Indian Ocean sediments, Quaternary Sci Rev, 17, 1185-1201, http://dx.doi.org/10.1016/S0277-3791(97)00099-1, 1998.

Stuiver, M., Reimer, P. J., Bard, E., Beck, J. W., Burr, G. S., Hughen, K. A., Kromer, B., McCormac, G., Van der Plicht, J., and Spurk, M.: INTCAL98 radiocarbon age calibration, 24,000-0 cal BP, Radiocarbon, 40, 1041-1083, 1998.

Suzuki, T.: Seasonal variation of the ITCZ and its characteristics over central Africa, Theor Appl Climatol, 103, 39-60, 10.1007/s00704-010-0276-9, 2011.

Talento, S., and Barreiro, M.: Simulated sensitivity of the tropical climate to extratropical thermal forcing: tropical SSTs and African land surface, Clim Dynam, 47, 1091-1110, 10.1007/s00382-015-2890-9, 2016.

Tarutani, T., Clayton, R. N., and Mayeda, T. K.: The effect of polymorphism and magnesium substitution on oxygen isotope fractionation between calcium carbonate and water, Geochim Cosmochim Ac, 33, 987-996, http://dx.doi.org/10.1016/0016-7037(69)90108-2, 1969.

Thomas, D. S. G., Bailey, R., Shaw, P. A., Durcan, J. A., and Singarayer, J. S.: Late Quaternary highstands at Lake Chilwa, Malawi: Frequency, timing and possible forcing mechanisms in the last 44ka, Quaternary Sci Rev, 28, 526-539, 2009.

Thomas, E. R., Wolff, E. W., Mulvaney, R., Steffensen, J. P., Johnsen, S. J., Arrowsmith, C., White, J. W. C., Vaughn, B., and Popp, T.: The 8.2ka event from Greenland ice cores, Quaternary Sci Rev, 26, 70-81, http://dx.doi.org/10.1016/j.quascirev.2006.07.017, 2007.

Thornalley, D. J. R., Elderfield, H., and McCave, I. N.: Holocene oscillations in temperature and salinity of the surface subpolar North Atlantic, Nature, 457, 711-714, 10.1038/nature07717, 2009.

Thrailkill, J.: Carbonate Deposition in Carlsbad Caverns, J Geol, 79, 683-695, 1971.

Tierney, J. E., Smerdon, J. E., Anchukaitis, K. J., and Seager, R.: Multidecadal variability in East African hydroclimate controlled by the Indian Ocean, Nature, 493, 389-392, 2013.

Tierney, J. E., and deMenocal, P. B.: Abrupt Shifts in Horn of Africa Hydroclimate Since the Last Glacial Maximum, Science, 342, 843, 2013.

Tierney, J. E., Russell, J. M., and Huang, Y.: A molecular perspective on Late Quaternary climate and vegetation change in the Lake Tanganyika basin, East Africa, Quaternary Sci Rev, 29, 787-800, http://dx.doi.org/10.1016/j.quascirev.2009.11.030, 2010.

Tierney, J. E., Russell, J. M., Huang, Y., Damsté, J. S. S., Hopmans, E. C., and Cohen, A. S.: Northern Hemisphere Controls on Tropical Southeast African Climate During the Past 60,000 Years, Science, 322, 252, 2008.

Timmermann, A., Lorenz, S. J., An, S. I., Clement, A., and Xie, S. P.: The Effect of Orbital Forcing on the Mean Climate and Variability of the Tropical Pacific, J Climate, 20, 4147-4159, 10.1175/JCLI4240.1, 2007.

Truc, L., Chevalier, M., Favier, C., Cheddadi, R., Meadows, M. E., Scott, L., Carr, A. S., Smith, G. F., and Chase, B. M.: Quantification of climate change for the last 20,000years from Wonderkrater, South Africa: Implications for the long-term dynamics of the Intertropical Convergence Zone, Palaeogeography, Palaeoclimatology, Palaeoecology, 386, 575-587, 2013.

Tudhope, A. W., Chilcott, C. P., McCulloch, M. T., Cook, E. R., Chappell, J., Ellam, R. M., Lea, D. W., Lough, J. M., and Shimmield, G. B.: Variability in the El Niño-Southern Oscillation Through a Glacial-Interglacial Cycle, Science, 291, 1511, 2001.

Vasey, N., Burney, D. A., and Godfrey, L.: Coprolites associated with Archaeolemur remains in North-western Madagascar suggest dietary diversity and cave use in a subfossil prosimian, in: Leaping Ahead: Advances in Prosimian Biology, edited by: Masters, J., Gamba, M., and Génin, F., Springer, New York, NY, 149–156, 2013.

Vecchi, G. A., and Soden, B. J.: Global Warming and the Weakening of the Tropical Circulation, J Climate, 20, 4316-4340, 10.1175/JCLI4258.1, 2007.

Vellinga, M., and Wood, R. A.: Global climatic impacts of a collapse of the Atlantic thermohaline circulation, Climatic Change, 54, 251-267, Doi 10.1023/A:1016168827653, 2002.

Venzke, S., Latif, M., and Villwock, A.: The Coupled GCM ECHO-2, J Climate, 13, 1371-1383, 10.1175/1520-0442(2000)013<1371:TCGE>2.0.CO;2, 2000.

Verschuren, D., Sinninghe Damste, J. S., Moernaut, J., Kristen, I., Blaauw, M., Fagot, M., and Haug, G. H.: Half-precessional dynamics of monsoon rainfall near the East African Equator, Nature, 462, 637-641, 2009.

Vinther, B. M., Buchardt, S. L., Clausen, H. B., Dahl-Jensen, D., Johnsen, S. J., Fisher, D. A., Koerner, R. M., Raynaud, D., Lipenkov, V., Andersen, K. K., Blunier, T., Rasmussen, S. O., Steffensen, J. P., and Svensson, A. M.: Holocene thinning of the Greenland ice sheet, Nature, 461, 385-388, 10.1038/nature08355, 2009.

Virah-Sawmy, M., Willis, K. J., and Gillson, L.: Evidence for drought and forest declines during the recent megafaunal extinctions in Madagascar, Journal of Biogeography, 37, 506-519, Doi 10.1111/J.1365-2699.2009.02203.X, 2010.

Virah-Sawmy, M., Willis, K. J., and Gillson, L.: Threshold response of Madagascar's littoral forest to sea-level rise, Global Ecol Biogeogr, 18, 98-110, 10.1111/j.1466-8238.2008.00429.x, 2009.

Voarintsoa, N. R. G., Brook, G. A., Liang, F., Marais, E., Hardt, B., Cheng, H., Edwards, R. L., and Railsback, L. B.: Stalagmite multi-proxy evidence of wet and dry intervals in northeastern Namibia: linkage to latitudinal shifts of the Inter-Tropical Convergence Zone and changing solar activity from AD 1400 to 1950, The Holocene, In press, 1-13, doi:10.1177/0959683616660170, 2017a.

Voarintsoa, N.R.G., Wang, L., Bruce Railsback, L., Brook, G.A., Liang, F., Cheng, H., Lawrence Edwards, R.: Multiple proxy analyses of a U/Th-dated stalagmite to reconstruct paleoenvironmental changes in northwestern Madagascar between 370 CE and 1300 CE. Palaeogeography, Palaeoclimatology, Palaeoecology 469, 138-155, 2017b.

Walker, M. J. C., Berkelhammer, M., Bjorck, S., Cwynar, L. C., Fisher, D. A., Long, A. J., Lowe, J. J., Newnham, R. M., Rasmussen, S. O., and Weiss, H.: Formal subdivision of the Holocene Series/Epoch: a Discussion Paper by a Working Group of INTIMATE (Integration of ice-core, marine and terrestrial records) and the Subcommission on Quaternary Stratigraphy (International Commission on Stratigraphy), J Quaternary Sci, 27, 649-659, 10.1002/jqs.2565, 2012.

Wang, L.: Late Quaternary paleoenvironmental changes in Southern Africa and Madagascar: evidence from aeolian, fluvial, and cave deposits, Unpub dissertation. University of Georgia, Athens, Georgia, 312pp, 2016.

Wang, L., Brook, G.A., 2013. Holocene Climate Changes in Northwest Madagascar: Evidence From a Two-meter-long Stalagmite From the Anjohibe Cave, Meeting Program of the Association of American Geographers, Published Online. Session 1512: Paleorecords of our Changing Earth I: Climate History and Human-Environment Interaction in the Old and New World Tropics, 2013.

Wang, X., Auler, A. S., Edwards, R. L., Cheng, H., Ito, E., Wang, Y., Kong, X., and Solheid, M.: Millennial-scale precipitation changes in southern Brazil over the past 90,000 years, Geophys Res Lett, 34, n/a-n/a, 10.1029/2007GL031149, 2007.

Wang, Y. J., Cheng, H., Edwards, R. L., He, Y. Q., Kong, X. G., An, Z. S., Wu, J. Y., Kelly, M. J., Dykoski, C. A., and Li, X. D.: The Holocene Asian monsoon: Links to solar changes and North Atlantic climate, Science, 308, 854-857, 10.1126/science.1106296, 2005.

Wanner, H., and Ritz, S. P.: A web-based Holocene Climate Atlas (HOCLAT): http://www.oeschger.unibe.ch/research/projects/holocene_atlas/, 2011.

Wanner, H., Beer, J., Butikofer, J., Crowley, T. J., Cubasch, U., Fluckiger, J., Goosse, H., Grosjean, M., Joos, F., Kaplan, J. O., Kuttel, M., Muller, S. A., Prentice, I. C., Solomina, O., Stocker, T. F., Tarasov, P., Wagner, M., and Widmann, M.: Mid- to Late Holocene climate change: an overview, Quaternary Sci Rev, 27, 1791-1828, 10.1016/j.quascirev.2008.06.013, 2008.

Wanner, H., Mercolli, L., Grosjean, M., and Ritz, S. P.: Holocene climate variability and change; a data-based review, J Geol Soc London, 172, 254-263, 10.1144/jgs2013-101, 2015.

Wanner, H., Solomina, O., Grosjean, M., Ritz, S. P., and Jetel, M.: Structure and origin of Holocene cold events, Quaternary Sci Rev, 30, 3109-3123, 10.1016/j.quascirev.2011.07.010, 2011.

Weaver, A. J., Bitz, C. M., Fanning, A. F., and Holland, M. M.: Thermohaline circulation: High-latitude phenomena and the difference between the Pacific and Atlantic, Annual Review of Earth and Planetary Sciences, 27, 231-285, DOI 10.1146/annurev.earth.27.1.231, 1999.

Webster, P. J., Moore, A. M., Loschnigg, J. P., and Leben, R. R.: Coupled ocean-atmosphere dynamics in the Indian Ocean during 1997-98, Nature, 401, 356-360, 1999.

Weldeab, S., Lea, D. W., Schneider, R. R., and Andersen, N.: 155,000 Years of West African Monsoon and Ocean Thermal Evolution, Science, 316, 1303, 2007.

Weller, E., and Cai, W. J.: Meridional variability of atmospheric convection associated with the Indian Ocean Dipole Mode, Sci Rep-Uk, 4, Doi 10.1038/Srep03590, 2014.

Wiersma, A. P., and Renssen, H.: Model–data comparison for the 8.2kaBP event: confirmation of a forcing mechanism by catastrophic drainage of Laurentide Lakes, Quaternary Sci Rev, 25, 63-88, http://dx.doi.org/10.1016/j.quascirev.2005.07.009, 2006.

Wiersma, A. P., Roche, D. M., and Renssen, H.: Fingerprinting the 8.2 ka event climate response in a coupled climate model, J Quaternary Sci, 26, 118-127, 10.1002/jqs.1439, 2011.

Williamson, D., Jelinowska, A., Kissel, C., Tucholka, P., Gibert, E., Gasse, F., Massault, M., Taieb, M., Van Campo, E., and Wieckowski, K.: Mineral-magnetic proxies of erosion/oxidation cycles in tropical maar-lake sediments (Lake Tritrivakely, Madagascar): paleoenvironmental implications, Earth Planet Sc Lett, 155, 205-219, http://dx.doi.org/10.1016/S0012-821X(97)00217-3, 1998.

Yamagata, T., Behera, S. K., Luo, J. J., Masson, S., Jury, M. R., and Rao, S. A.: Coupled ocean-atmosphere variability in the tropical Indian Ocean: Earth's Climate, The Ocean-Atmosphere Interaction, 147, 189-211, 2004.

Yan, H., Wei, W., Soon, W., An, Z., Zhou, W., Liu, Z., Wang, Y., and Carter, R. M.: Dynamics of the intertropical convergence zone over the western Pacific during the Little Ice Age, Nature Geosci, 8, 315-320, 10.1038/ngeo2375, 2015.

Zhang, H.-L., Yu, K.-F., Zhao, J.-X., Feng, Y.-X., Lin, Y.-S., Zhou, W., and Liu, G.-H.: East Asian Summer Monsoon variations in the past 12.5ka: High-resolution δ18O record from a precisely dated aragonite stalagmite in central China, J Asian Earth Sci, 73, 162-175, 2013.

Zhang, H., Cai, Y., Tan, L., Qin, S., and An, Z.: Stable isotope composition alteration produced by the aragonite-to-calcite transformation in speleothems and implications for paleoclimate reconstructions, Sediment Geol, 309, 1-14, 2014.

Zhang, R., and Delworth, T. L.: Simulated tropical response to a substantial weakening of the Atlantic thermohaline circulation, J Climate, 18, 1853-1860, Doi 10.1175/Jcli3460.1, 2005.

Zheng, W., Braconnot, P., Guilyardi, E., Merkel, U., and Yu, Y.: ENSO at 6ka and 21ka from ocean–atmosphere coupled model simulations, Clim Dynam, 30, 745-762, 10.1007/s00382-007-0320-3, 2008.

Zheng, X.-T., Xie, S.-P., Du, Y., Liu, L., Huang, G., and Liu, Q.: Indian Ocean Dipole Response to Global Warming in the CMIP5 Multimodel Ensemble, J Climate, 26, 6067-6080, 10.1175/JCLI-D-12-00638.1, 2013.

Zinke, J., Dullo, W. C., Heiss, G. A., and Eisenhauer, A.: ENSO and Indian Ocean subtropical dipole variability is recorded in a coral record off southwest Madagascar for the period 1659 to 1995, Earth Planet Sc Lett, 228, 177-194, 10.1016/j.epsl.2004.09.028, 2004.

Figures

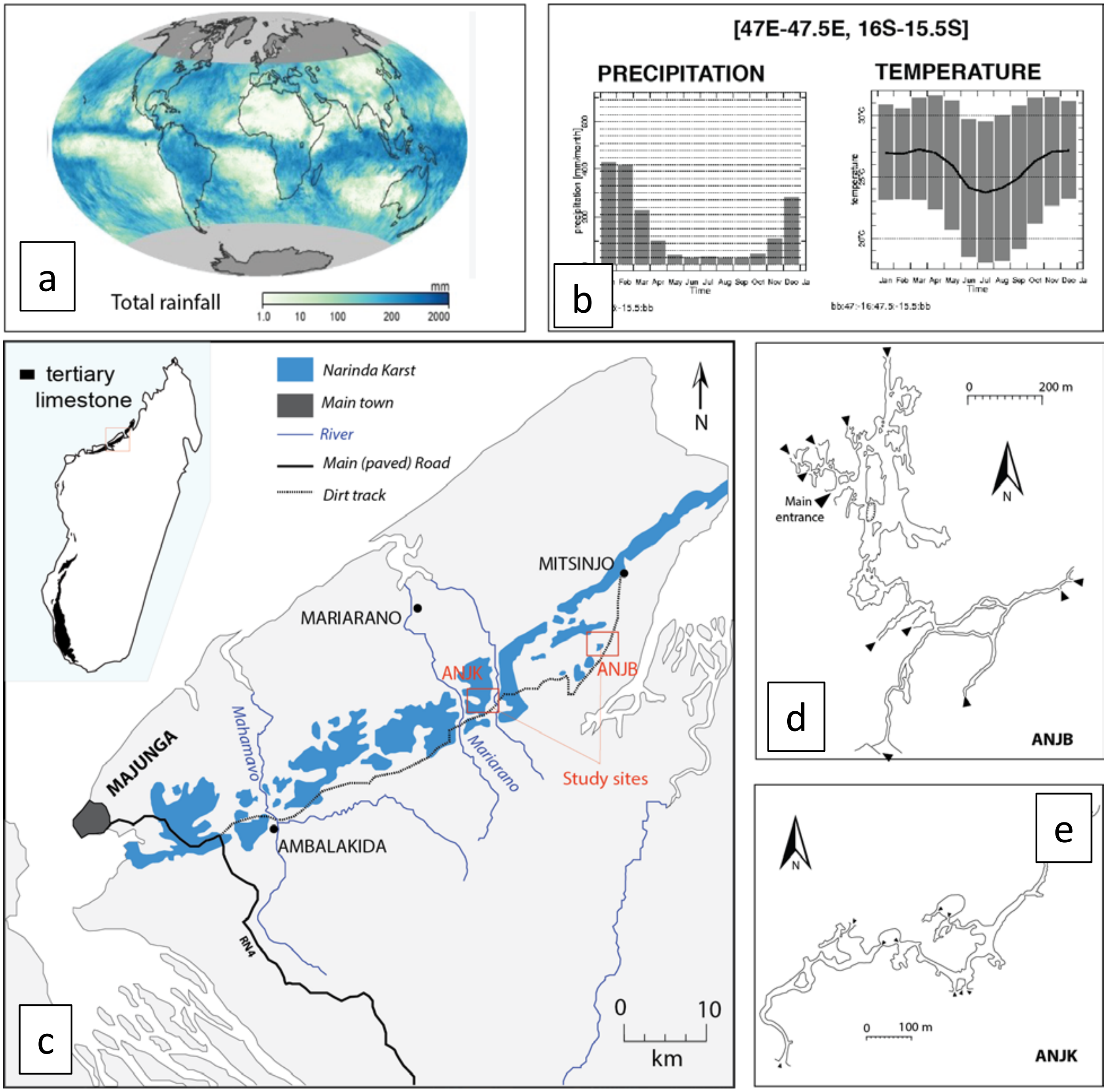

Figure 1: **Climatological and geographic setting of Madagascar and the study area**. (a) Global rainfall maps recorded by NASA's Tropical Rainfall Measuring Mission (TRMM) satellite showing the total monthly rainfall in millimeters and the overall position of the ITCZ during November, 2006. Darker blue shades indicate regions of higher rainfall (source: NASA Earth Observatory, 2016). (b) Barplots of the monthly climatology of precipitation, and the monthly average of daily maximum, minimum, and mean temperature in NW Madagascar. The base period used for the climatology is 1971-2000. Source: http://iridl.ldeo.columbia.edu/ (accessed August 31, 2016). (c)

Simplified map showing the southwest part of the Narinda karst and the location of the study areas. Inset figure is a map of Madagascar showing the extent of the Tertiary limestone cover that makes up the Narinda karst. (d-e) Maps of Anjohibe (ANJB) and Anjokipoty (ANJK) caves (St-Ours, 1959; Middleton and Middleton, 2002). See Figs. S1–S3 for additional information about the study locations.

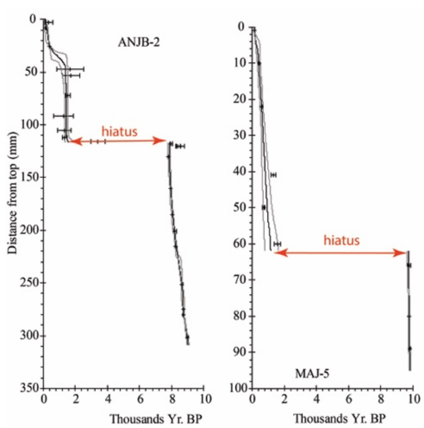

Figure 2: **Age model of Stalagmite ANJB-2 and MAJ-5** using the StalAge1.0 algorithm of Scholz and Hoffman (2011) and Scholz et al. (2012).

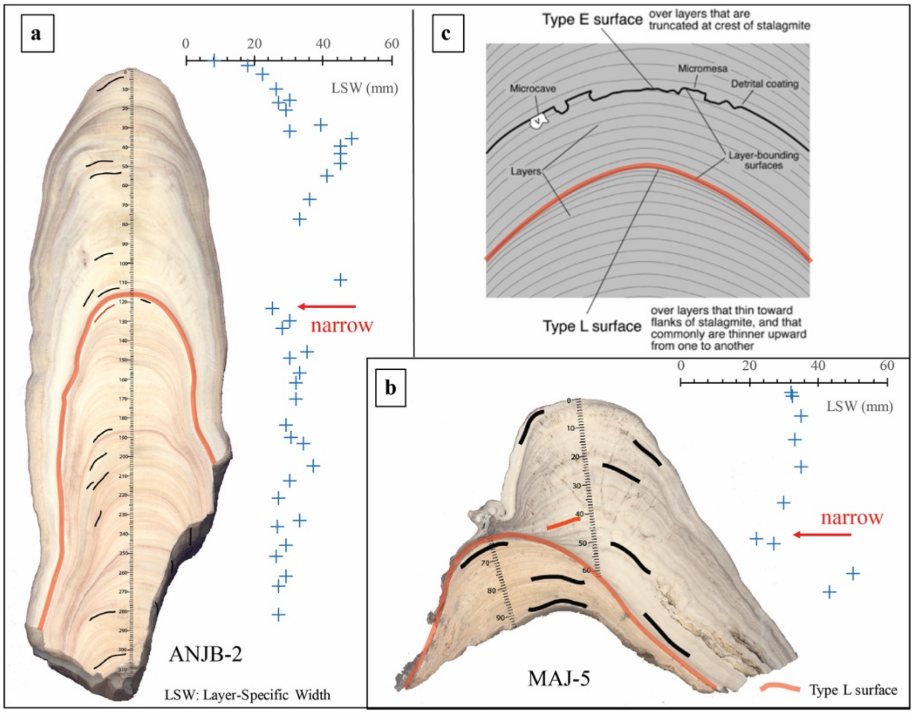

Figure 3: a) Scanned image of Stalagmite ANJB-2 and the corresponding variations in layer-specific width (LSW). b) Scanned image of Stalagmite MAJ-5 and the corresponding layer-specific width (LSW). c) Sketches of typical layer-bounding surfaces (Type E and Type L) of Railsback et al. (2013). Close-up of photographs of the hiatuses are shown in Fig S6.

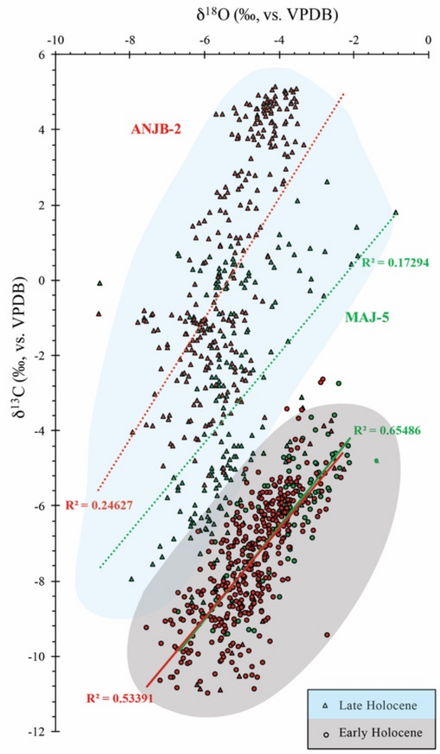

Figure 4: **Stable isotope data**. Scatterplots of $\delta^{13}C$ and $\delta^{18}O$ for Stalagmite MAJ-5 (green) and ANJB-2 (red) during the Malagasy early Holocene interval (circle) and the Malagasy late Holocene interval (triangle). The plot shows distinctive early and late Holocene conditions (roughly highlighted in gray and light blue shade, respectively).

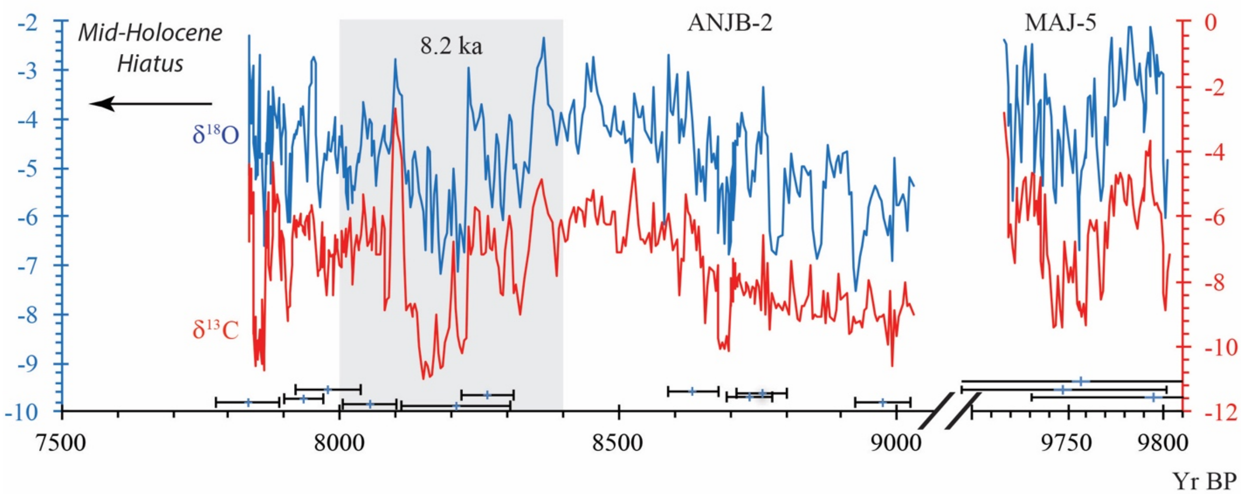

Figure 5: Variations in $\delta^{13}C$ and $\delta^{18}O$ in Stalagmite ANJB-2 and Stalagmite MAJ-5 during the Malagasy Early Holocene Interval. Supplementary Fig. S6 shows both the corrected and uncorrected values.

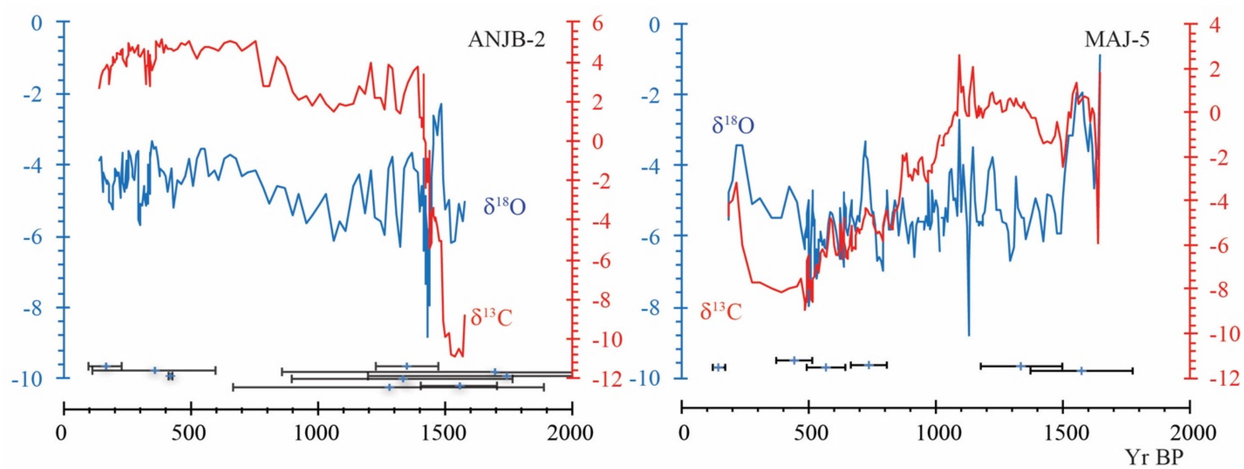

Figure 6: Variations in $\delta^{13}C$ and $\delta^{18}O$ in Stalagmite ANJB-2 and Stalagmite MAJ-5 during the Malagasy Late Holocene Interval. Supplementary Fig. S7 shows both the corrected and uncorrected values, and Fig. S8 compares the corrected $\delta^{18}O$ for both stalagmites.

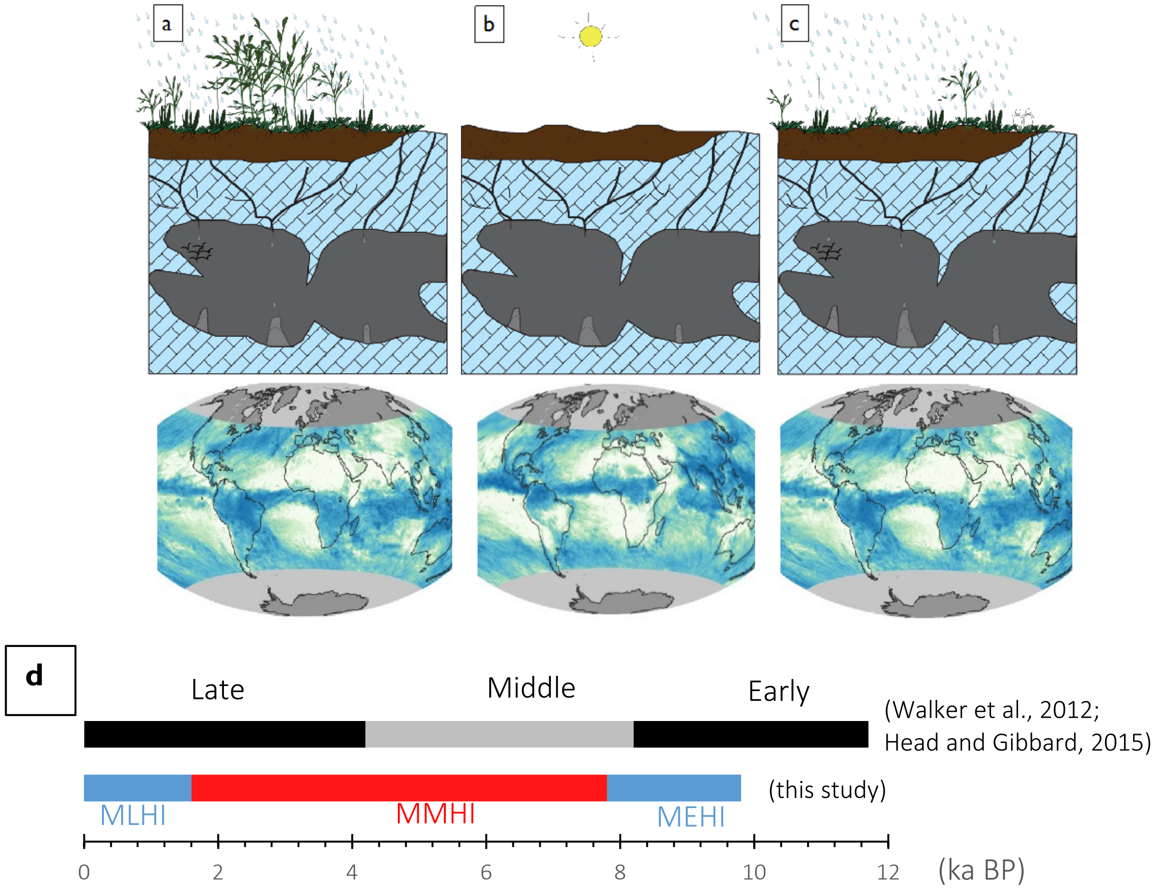

Figure 7: **Simplified models portraying the Holocene climate change in NW Madagascar and the possible climatic conditions linked to the ITCZ**. a) Wetter conditions during the early Holocene with ITCZ south (prior to c 7.8 ka), favorable for stalagmite deposition. b) Periodic dry conditions during the mid-Holocene (between c. 7.8 and 1.6 ka) with ITCZ north with no stalagmite formation (refer to Sect. 5.2.2). c) Wetter conditions during the late Holocene (after c. 1.6 ka) with ITCZ south, favorable for stalagmite deposition. For details about paleo-vegetation reconstruction. Drawings are not to scale. The bottom figures are from the same source as Fig. 1a, and they are only used here to give a perspective of the possible position of the ITCZ during the early, mid, and late Holocene. d) Comparison of the three Malagasy Holocene interval with the Walker et al. (2012) and Head and Gibbard (2015) subdivision (see text for details, Sect. 5.2).

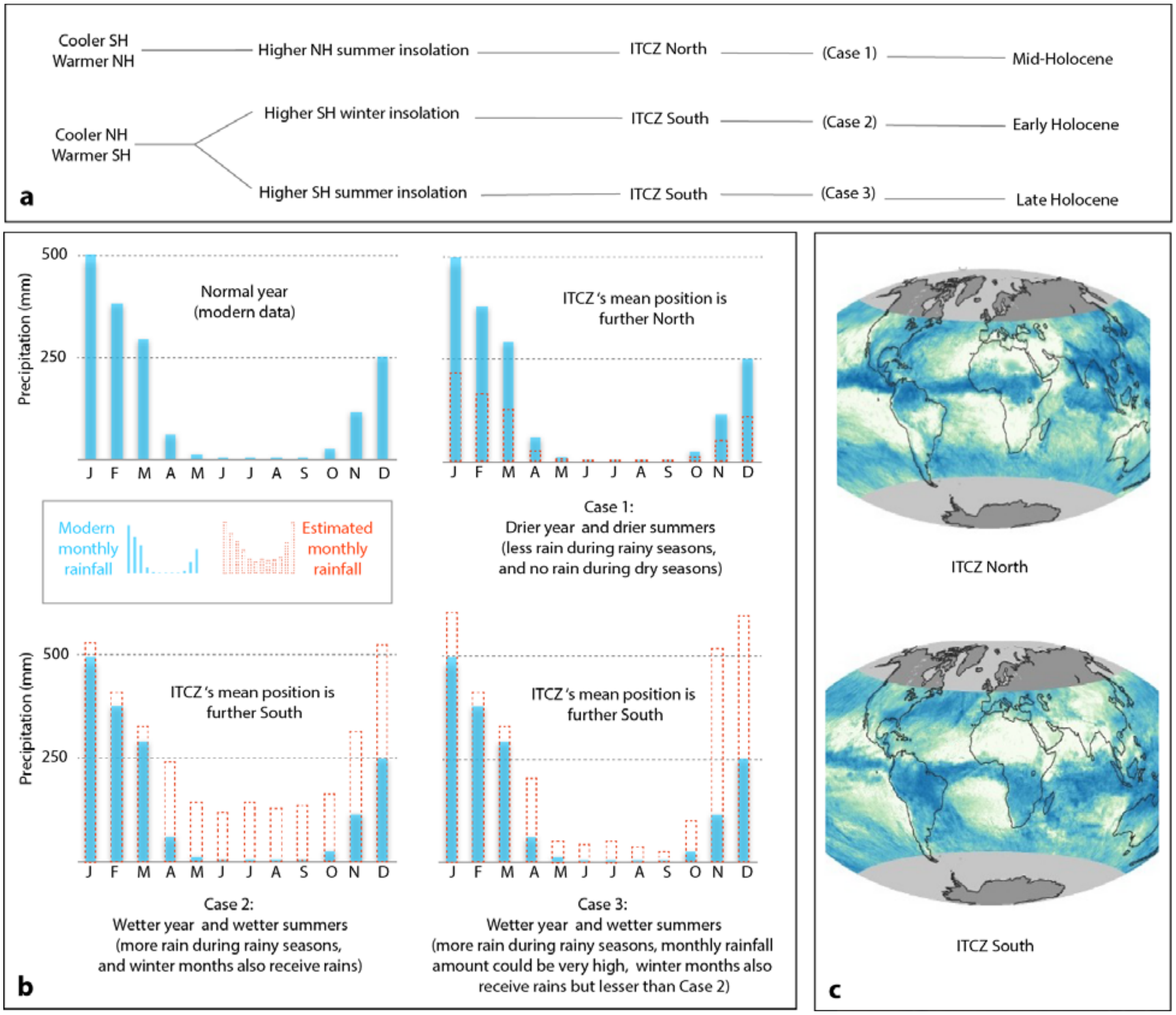

Figure 8: **Conceptualizing the different possible outcomes of the long-term latitudinal migration of the ITCZ**. a) Highlighting the three possible scenarios of the Holocene. b) Barplots of monthly rainfall in NW Madagascar, using the modern data as a reference to estimating the region's paleoclimate during drier and wetter conditions. c) Global rainfall maps from NASA (same source as Fig.1). These maps are modern, but they are only shown here to give a better perspective of the position of Madagascar when the ITCZ is relatively north or south. See supplementary text for details.

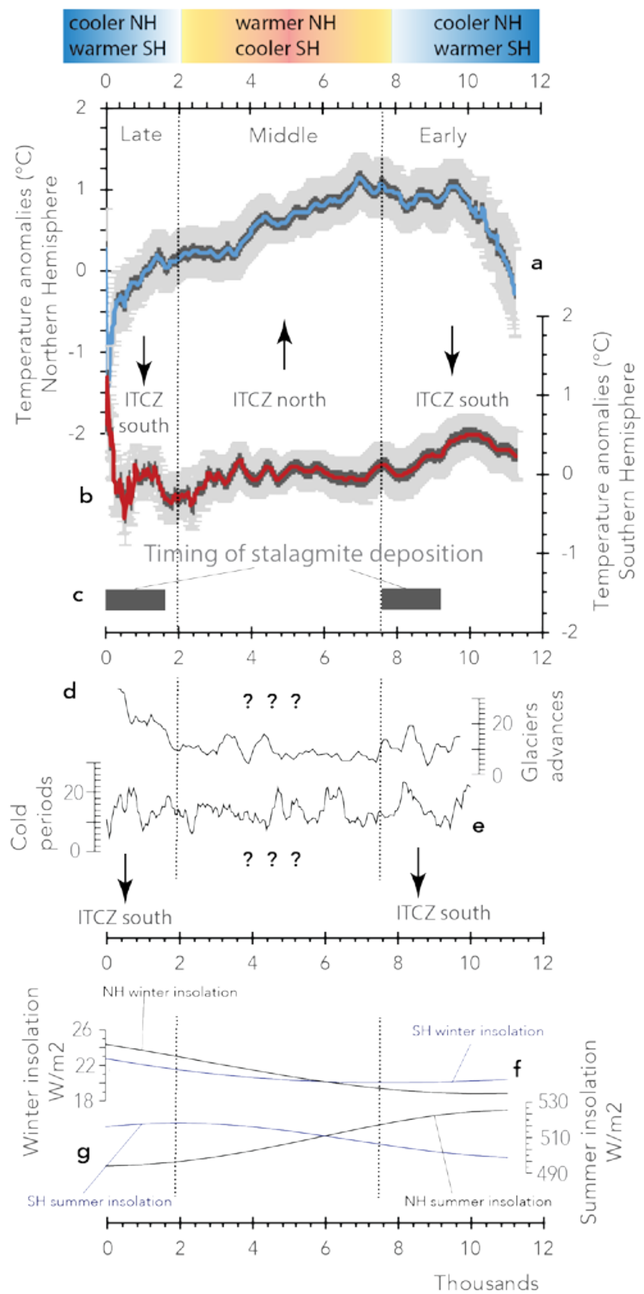

Figure 9: **Possible Holocene climate forcings that influenced climate of NW Madagascar**. a) Average Holocene temperatures in the NH 90°–30°N (blue). b) Average Holocene temperatures in the SH 90°–30°S (red). These temperature data are referenced to the 1961–1990 mean temperature (Marcott et al., 2013), with 1σ uncertainty (gray). c) Timing of deposition of Stalagmite ANJB-2 and MAJ-5. d) Curves representing the sum of glaciers advances from a set of global Holocene time series compiled from natural paleoclimate archives (Wanner et al., 2011). e) curves representing the sum of cold periods from a set of global Holocene time series

compiled from natural paleoclimate archives (Wanner et al., 2011). f) Winter insolation curves (Berger and Loutre, 1991). G) Summer insolation curves (Berger and Loutre, 1991)

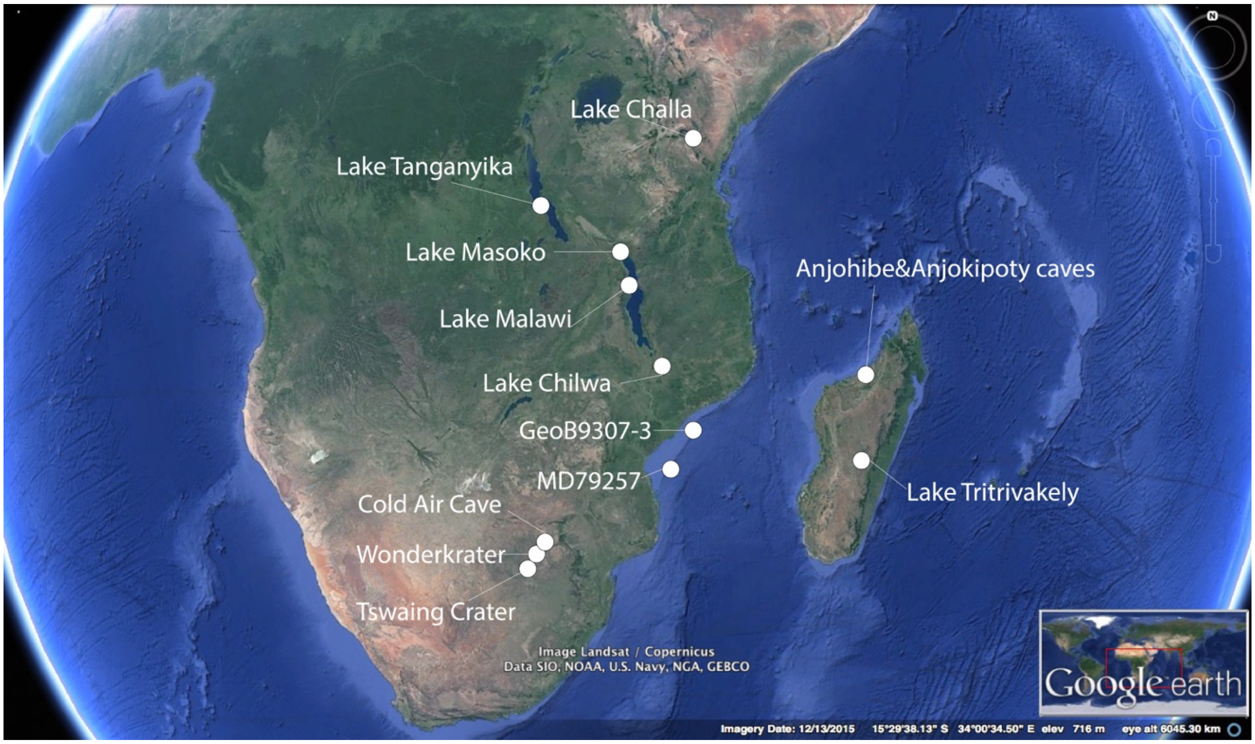

Figure 10: Regional comparison. Google Earth image showing the location of the sites reported in Table S3 and in Figure 11. Most records reported from these sites are lake sediments, except for GeoB9307-3 (onshore off delta sediments), MD79257 (alkenone from marine sediment core), and Cold Air, Anjohibe, and Anjokipoty caves (stalagmites $\delta^{18}O$).

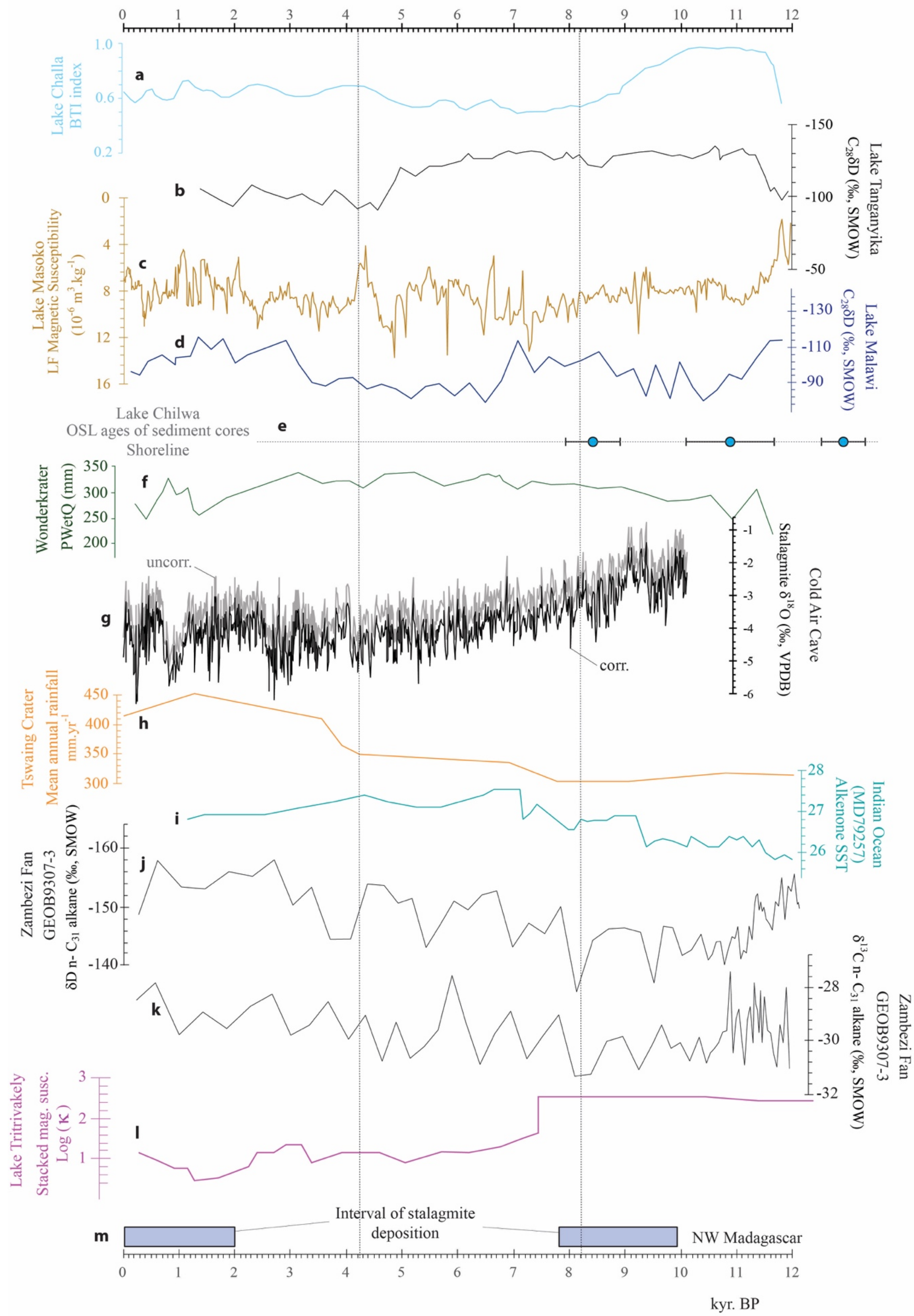
Lake Challa BTI index
a
Lake Tanganyika C28δD (‰, SMOW)
b
Lake Masoko LF Magnetic Susceptibility (10-6 m3.kg-1)
c
Lake Malawi C28δD (‰, SMOW)
d
Lake Chilwa OSL ages of sediment cores Shoreline
e
Wonderkrater PWetQ (mm)
f
uncorr.
corr.
Cold Air Cave Stalagmite δ18O (‰, VPDB)
g
Tswaing Crater Mean annual rainfall mm.yr-1
h
Indian Ocean (MD79257) Alkenone SST
i
Zambezi Fan GEOB9307-3 δD n- C31 alkane (‰, SMOW)
j
Zambezi Fan GEOB9307-3 δ13C n- C31 alkane (‰, SMOW)
k
Lake Tritrivakely Stacked mag. susc. Log (K)
l
Interval of stalagmite deposition
NW Madagascar
m
kyr. BP

Figure 11: Regional comparison. a) Lake Challa BTI index (Verschuren et al., 2009). b) Lake Tanganyika C_{28} δD (Tierney et al., 2008, 2010). c) Lake Masoko low field magnetic susceptibility ($10^{-6}.m^3kg^{-1}$) (Garcin et al., 2006). d) Lake Malawi C_{28} δD (Konecky et al., 2011). e) Lake Chilwa OSL dates of shoreline (Thomas et al., 2009). f) Wonderkrater reconstructed paleoprecipitation, PWetQ (Precipitation of the Wettest Quarter; Truc et al., 2013). g) Cold Air Cave corrected (corr.) and uncorrected (uncorr.) $\delta^{18}O$ profiles from Stalagmite T8 (Holmgren et al., 2003). h) Tswaing Crater paleo-rainfall derived from sediment composition (Partridge et al., 1997). i) Indian Ocean SST records from alkenone (Bard et al., 1997; Sonzogni et al., 1998). j-k) Zambezi δD n-C_{31} alkane $\delta^{13}C$ n-C_{31} alkane (Schefuß et al., 2011). l) Lake Tritrivakely stacked magnetic susceptibility (Williamson et al., 1998). m) NW Madagascar (Anjohibe and Anjokipoty) interval of deposition of Stalagmite ANJB-2 and Stalagmite MAJ-5 (this study). The two vertical dashed lines indicate the boundary of the Early, Middle, and Late Holocene by Walker et al. (2012) and Head and Gibbard (2015).

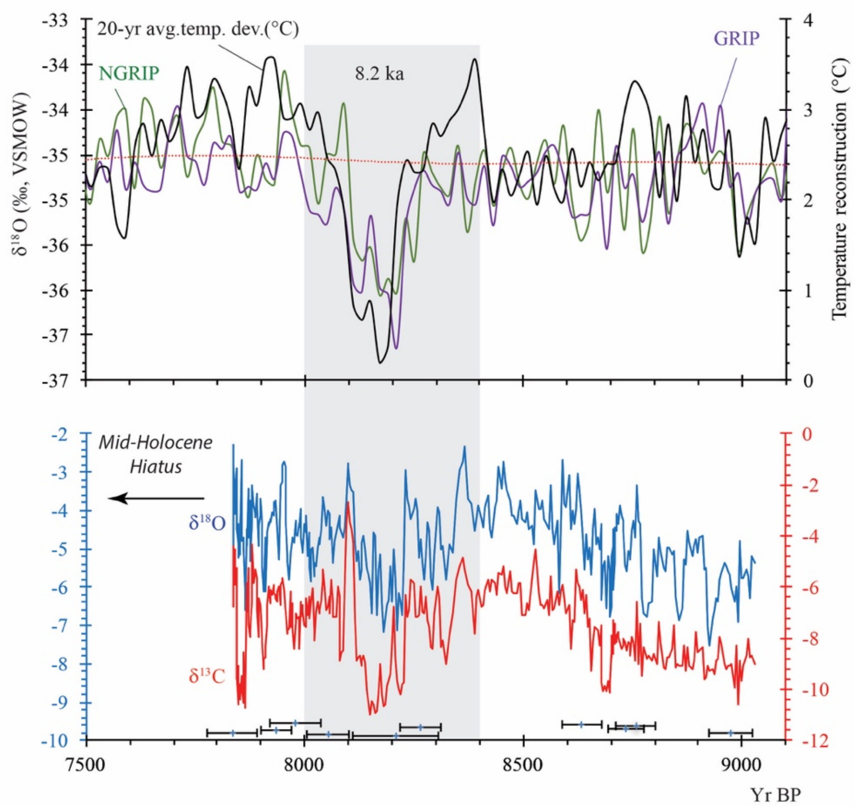

Figure 12: **The 8.2 ka event in Madagascar**. Oxygen isotope record from Greenland (GRIP and NGRIP) ice cores (Vinther et al., 2009) compared with Stalagmite ANJB-2 $\delta^{18}O$ and $\delta^{13}C$.